Olli Kuusisto

The Effects of Installation-Based Defects in Medium Voltage Cable Joints

Helsinki Metropolia University of Applied Sciences

Bachelor of Engineering

Electrical Power Engineering

Thesis

March 15, 2016

Author Title Number of Pages Date	Olli Kuusisto The Effects of Installation-Based Defects in Medium Voltage Cable Joints 54 pages + 4 appendices 15 March 2016
Degree	Bachelor of Engineering
Degree Programme	Electrical Engineering
Specialisation option	Electrical Power Engineering
Instructors	Timo Vikman, Product Development Manager Tuomo Heikkinen, Senior Lecturer

A cable joint is a common accessory which is used to connect the underground cables. In the medium voltage networks, a high percentage of the faults occur on the cable accessories. It is very expensive to repair these breakdowns, so the network companies are interested to prevent premature breakdowns.

This bachelor's thesis was commissioned by Ensto Finland Oy. The purpose of this thesis was to study, how the installation-based defects affect the medium voltage cable joints. The studied joints were Ensto's heat and cold shrink joints for 12/20 (24) kV cables with XLPE insulation and copper wire shield. The cable joints for the other cable types were not studied because the general structure is similar in all joint types. The effects of the defects were only studied on one cable size.

The effects of the installation-based defects were studied first by simulating. The partial discharge inception voltages of few fault types were calculated with the help of a simulation program. The partial discharge inception voltages were measured in the laboratory tests on real joints to verify the simulation results. The tests also produced further information about the seriousness of the fault. COMSOL Multiphysics was used as the simulation program. The electrical tests were offline partial discharge test and AC voltage step. The partial discharge inception and extinguishing voltages and discharge levels were measured in the partial discharge test. The purpose of the AC voltage step test was to give information about the weakest point in tested joints.

As a result of this thesis, the most critical defect types were evaluated. The results will be used in Ensto Pro training materials.

Keywords	Medium voltage, underground cable, cable joint, electric field, simulation, partial discharge, electric breakdown

Tekijä Otsikko Sivumäärä Aika	Olli Kuusisto Asennusvirheistä johtuvien vikojen vaikutus keskijännitekaapelijatkoksissa 54 sivua + 4 liitettä 15.3.2016
Tutkinto	Insinööri (AMK)
Koulutusohjelma	Sähkötekniikka
Suuntautumisvaihtoehto	Sähkövoimatekniikka
Ohjaajat	Product Development Manager Timo Vikman Lehtori Tuomo Heikkinen

Kaapelijatkos on yleinen varuste, jota käytetään maakaapeleiden yhdistämiseen. Keskijänniteverkoissa suuri osa käyttökatkon aiheuttamista vaurioista tapahtuu kaapelivarusteissa. Rikkoutumisten korjaaminen on yleensä erittäin kallista, joten verkkoyhtiöt ovat kiinnostuneita ennenaikaisten läpilyöntien ennaltaehkäisemisestä.

Tämä insinöörityö tehtiin Ensto Finland Oy:n toimeksiannosta. Työn tarkoituksena oli tutkia, kuinka asennusvirheistä johtuvat viat vaikuttavat keskijännitekaapeleissa. Työssä tutkitut jatkokset olivat Enston lämpö- ja kylmäkutistejatkoksia PEX-eristeellä ja kuparilankasuojalla varustetuille 12/20 (24) kV -kaapeleille. Kaapelijatkoksia muille kaapelityypeille ei tutkittu, koska kaikkien jatkosten rakenne on pääpiirteittäin samanlainen. Työssä tutkittiin vikojen vaikutuksia ainoastaan yhdellä kaapelikoolla.

Asennusvirheiden vaikutuksia tutkittiin aluksi simuloimalla. Simulointituloksien perusteella laskettiin osittaispurkauksien syttymisjännitteet eri virhetyypeille. Simulointitulosten varmistamiseksi osittaispurkausten syttymisjännitteet mitattiin laboratoriotesteissä todellisilla jatkoksilla. Testeillä tuotettiin myös lisäinformaatiota vikojen vakavuudesta. Työssä käytetty simulointiohjelma oli COMSOL Multiphysics. Laboratoriotestit olivat offline-osittaispurkausmittaus ja portaittainen AC-jännitetesti. Osittaispurkausmittauksessa mitattiin osittaispurkauksien syttymis- ja sammumisjännitteet sekä purkaustasot. Portaittaisen AC-jännitetestin tarkoituksena oli antaa informaatiota testatun jatkoksen heikoimmasta kohdasta.

Tämän työn tuloksena saatiin arvioitua vikatyypit, jotka ovat kriittisimpiä jatkoksen eliniän kannalta. Työn tuloksia tullaan hyödyntämään Ensto Pro -koulutuksien materiaalissa.

Avainsanat	Keskijännite, maakaapeli, kaapelijatkos, sähkökenttä, simulointi, osittaispurkaus, läpilyönti

Preface

This study was made for Utility Networks of Ensto Finland Oy. I would like to thank everyone who participated in this project.

Especially I would like to thank my supervisors, Tuomo Heikkinen and Timo Vikman for the guidance. I also would like to thank Product Manager Kauko Alkila for this subject and for all his help. For all the technical support and help, I would like to thank Technical Manager Kenneth Väkeväinen and Product Development Engineer Anssi Aarnio. For performing the electrical tests, I would like to thank Laboratory Engineer Sampo Vuokkiniemi.

Porvoo, March 15, 2016

Olli Kuusisto

Contents

Abbreviations and Symbols

ε	Permittivity
ε_0	Vacuum permittivity
ε_r	Relative permittivity
σ	Surface charge density, also electrical conductivity
Φ	Electric flux
C	Coulomb, SI unit of electric charge, also capacitance
CSM	Charge simulation method
E	Electric field
E_b	Dielectric breakdown strength
E_{max}	Dielectric strength
e	Elementary charge
F	Force
FEM	Finite element method
J	Joule, SI unit of energy
N	Newton, SI unit of force
PD	Partial discharge
PDIV	Partial discharge inception voltage
PVC	Polyvinyl chloride

Q	Electric charge
SI	International System of Units (French: Système international d'unités)
U_0	Phase voltage
U_e	Extinguishing voltage
U_E	Electric potential energy
U_i	Inception voltage
U_m	Maximum voltage
XLPE	Cross-linked polyethylene, also known as PEX

1 Introduction

The use of underground cables continues to grow as a result of urbanization and demands for trouble-free distribution. Concern over installation quality has emerged as the amount of underground cable lines increases. When some disassembled cable accessories have been opened up, in the worst cases, as many as half of the accessories have showed signs of installation-based defects. Network companies are interested of improving the quality of underground installation work because repairing underground lines is generally more expensive and slower than repairing overhead lines. [1]

Ensto is also, as a cable accessory manufacturer, interested of improving installation quality and reliability of underground networks. Because of this Ensto offers its customers Ensto Pro product trainings which include both theory-based lessons and practical installation exercises. The main goal of the trainings is to reduce the amount of installation errors, and thereby ensure a long service life and reliable operation. [1]

The aim of this thesis was to study how the installation-based defects affect medium voltage cable joints and to provide material that can be used in Ensto Pro trainings. The joints were chosen to be studied because they are more expensive to repair than cable terminations, since they are mainly installed underground. The examined joint types were Ensto's heat and cold shrink joints for single core 12/20 (24) kV cables with XLPE insulation and copper wire shield. Cable joints for other medium voltage cable types were not studied since the general structure is similar in all joints that are designated for XLPE insulated cables. The use of a polymeric insulated cable was chosen because they are more common today than any other cable types.

The study was carried out by first studying the theory behind the breakdown phenomenon on solid insulations. Then different fault types were studied with a simulation program. Same fault types were also tested on actual joints in the laboratory tests to verify the simulation results and to produce further information about the seriousness of the fault. The reliability of the simulation results were also evaluated in this thesis.

2 Electrostatics

In order to understand the results and analysis in this work, some sort of knowledge of electrostatics is required. Electrostatics is a branch of physics which deals with the phenomena and events of stationary or slow-moving electric charges. [2, 7]

2.1 Electric Charge

Electric charge is an intrinsic property of the protons and the electrons. The absolute value of the electron and proton charge is the elementary charge *e*. The elementary charge is a fundamental physical constant and its value is approximately 1.602 176 x 10^{-19} C. The proton has a charge of +*e*, and the electron has a charge of -*e*. The charges of particles are always a multiple of the elementary charge. The SI unit of electric charge is the coulomb (C) and the symbol is *Q*. The SI system defines the coulomb in terms of the ampere and second. One coulomb is the charge transported by a constant current of one ampere in one second, i.e. 1 C = 1 As. [2, 7; 3, 11]

2.2 Coulomb's Law

Coulomb's law states that "the electrical force between two charged objects is directly proportional to the product of the charges and inversely proportional to the square of the separation distance between the two objects". In the presence of a dielectric between two charges, the Coulomb's law can be expressed as

$$F = \frac{k}{\varepsilon_r} * \frac{|Q_1 Q_2|}{r^2}, \qquad (1)$$

where ε_r is relative permittivity of the dielectric medium and *k* is the constant of proportionality. The value of *k* is

$$k = \frac{1}{4\pi\varepsilon_0} = 8.98755 * 10^9 \frac{Nm^2}{C^2}, \qquad (2)$$

where ε_0 is the permittivity of free space. The SI value of ε_0 is 8.85×10^{-12} C^2/Nm^2. [2, 8; 3, 28-29]

2.3 Electric Field

An electric field *E* is defined as being present in a point where a charged object experiences the electric force. In other words, the electric field at the specific point is the force per unit charge that the charge would experience at that point, i.e.

$$E = \frac{F}{Q} \tag{3}$$

The SI unit of the electric field is N/C or equivalently V/m. The field can be represented by vectors as Figure 1a shows. The field exists at every point in space, but in the picture each vector represents the field at only one point. The field can be visualized also by drawing electric field lines as Figure 1b illustrates. [4, 34]

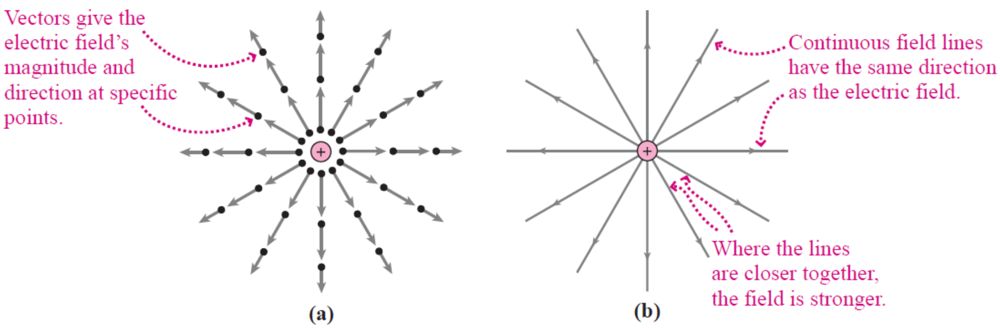

Figure 1. Electric field visualized by vectors (a) and field lines (b). Copied from Wolfson (2014) [4, 34].

The field lines begin on positive charges and end on negative charges. The electric field exists everywhere, so there is actually infinite number of field lines. On the field line pictures the amount of the field lines is associated with charge of given magnitude *Q*. The strength of the electric field of the point charge can be calculated at any point with the help of Coulomb's law:

$$E = \frac{F}{q} = \frac{k * \frac{qQ}{r^2}}{q} = k * \frac{Q}{r^2}\ , \tag{4}$$

where r is the distance from point charge. Usually field direction varies, so the lines are curved as Figure 2 shows a number of dipole field lines. [3, 32; 4, 34]

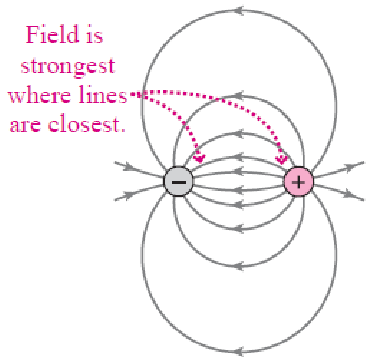

Figure 2. Several field lines showing the overall dipole field. Copied from Wolfson (2014) [4, 34].

With the help of Gauss's law, the electric field of more complicated, but sufficiently symmetrical, charge distribution can be calculated easier. Gauss's law states that "the electric flux through any closed surface is equal to the total charge enclosed by that surface", i.e.

$$\Phi = \oint \vec{E} * d\vec{A} = \frac{Q_{enclosed}}{\varepsilon_0}, \quad (5)$$

where Φ is the electric flux through a closed surface A and $Q_{enclosed}$ is net charge enclosed by surface A. In other words, the electric flux describes the amount of electric field crossing the area [2, 15; 4, 49]

2.4 Electric Potential

The work done in the moving charged particle against the electric force is stored as an electric potential energy U_E. The SI unit of electric potential energy is the joule (J). An electric potential V is the electric potential energy of the charged particle at any location divided by the charge of that particle, i.e.

$$V = \frac{U_E}{Q} \quad (6)$$

Since the charge of the particle has been divided out, the electric potential is a property of the electric field itself and not related to the charged particle. The SI unit for electric potential is joules per coulomb (J/C). The unit also has its own name, the volt (V). In the electric fields, the potential difference varies linearly with the distance. With the equipotential lines potential differences can be drawn as Figure 3 shows. These lines are determined by points at the same electric potential. [4, 56-57 & 64-65]

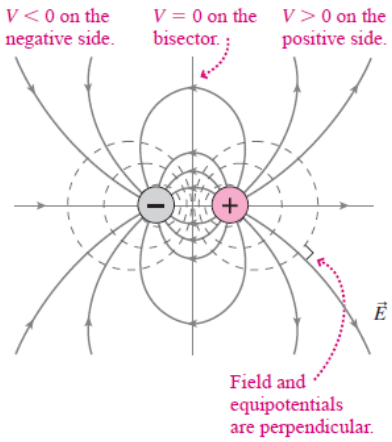

Figure 3. The field lines and equipotential lines (dashed curves) around an electric dipole. Copied from Wolfson (2014) [4, 65].

The electric field lines are always perpendicular to the equipotential lines. So the electric field can be drawn if the equipotential lines are known, or vice versa. [4, 65]

2.5 Matter in Electric Fields

In terms of the electrostatics, materials can be divided into insulators and conductors. The key difference between insulators and conductors is the mobility of charges. In conductors, the individual charges are free to move throughout the materials. In insulators, internal charges are fixed in one location. [4, 22]

2.5.1 Conductor in Electric Field

When the electric field is applied to the conductor, free charges respond to the electric force. The positive charges respond by moving in the direction of the field and the negative charges respond by moving in the opposite direction of the field. The movement of charges creates an electric field within the conductor that is opposite to the applied field. As more charges move, the magnitude of the internal field increases until it is equal to the applied field. At that point, the conductor is in electrostatic equilibrium, and the charges within the conductor experience zero net force and the electric field is zero inside the conductor. [4, 45]

In electrostatic equilibrium there cannot be an electric field within a conductor, but there may be a field right at the conductor surface. The field of a charged conductor is perpendicular to the surface and the magnitude is

$$E = \frac{\sigma}{\varepsilon_0}, \tag{7}$$

where σ is a surface charge density. [4, 47]

2.5.2 Insulator in Electric Field

In insulators charges are bound into neutral molecules. When a dielectric object is brought to the electric field, the charges in each molecule move so that the focus of the positive and negative charges separate from each other and molecules acquire induced dipole moments as Figure 4 shows. Some dielectric molecules, like water molecules, have intrinsic dipole moments. [4, 22-23]

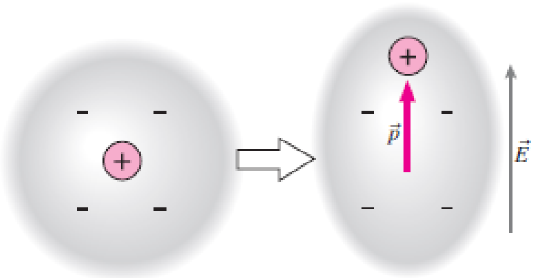

Figure 4. The charges of molecule respond to an electric field. Copied from Wolfson (2014) [4, 23].

In the applied electric field, the molecular dipoles experience a torque that tends to align them with the polarity of the field. The internal electric fields of the dipoles, pointing from their positive to their negative charges, then reduces the applied electric field within the object as Figure 5 shows. [4, 23]

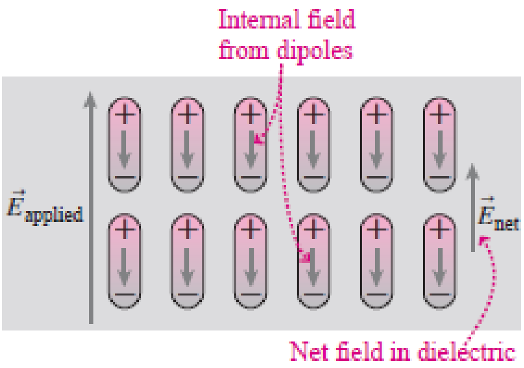

Figure 5. The alignment of molecular dipoles in the electric field. Copied from Wolfson (2014) [4, 23].

This phenomenon is called a dielectric polarization. The ability of material to polarize can be described with a measure called permittivity ε. The permittivity is the measure of how the electric field is affected by the dielectric medium. Relative permittivity ε_r, where the permittivity of insulator is expressed as a ratio relative to the permittivity of vacuum ε_0, is more commonly used. [5, 20]

With alternating current, the polarity of the electric field alternates. As a result, the molecular dipoles are in constant rotation that heats the insulation as a result of friction. This heating may lead to a thermal breakdown of the insulation. The energy losses which go into this heating are called dielectric losses. These dielectric losses are proportional to the frequency and thereby the thermal breakdowns are more likely at high frequencies. [5, 51 & 127]

If the applied electric field is too great, the individual charges are ripped free from the dielectric and the material starts acting as a conductor. This phenomenon is called an electrical breakdown. Dielectric strength E_{max} is the maximum value of the electric field that the insulator can withstand under ideal conditions without breaking down. The SI unit for dielectric strength is volts per meter, V/m. [2, 17; 4, 23]

3 Breakdown in Solid Insulation

The electrical breakdown is defined as an abrupt increase in the electric current flowing through the dielectric. The breakdown is caused by the energy provided by the electric field that can be transferred by collision ionization (electrical breakdown) or by thermal losses (thermal breakdown). Breakdown leads to thermal destruction of insulator and in solid insulation destruction causes permanent loss of insulating properties. [5, 124]

An ideal insulator does not exist as all the materials contain charge carriers. The leakage current increases exponentially when the voltage stress is increased close to the breakdown of the insulator. The increase of the leakage current is assumed to be caused by increasing number of the charge carriers in the insulation and the electrode surfaces. Breakdown process is affected also by other factors, such as the leakage current and the dielectric losses causing the heat, the electrostatic forces, the electrochemical reactions, the water trees and the erosion. [5, 124]

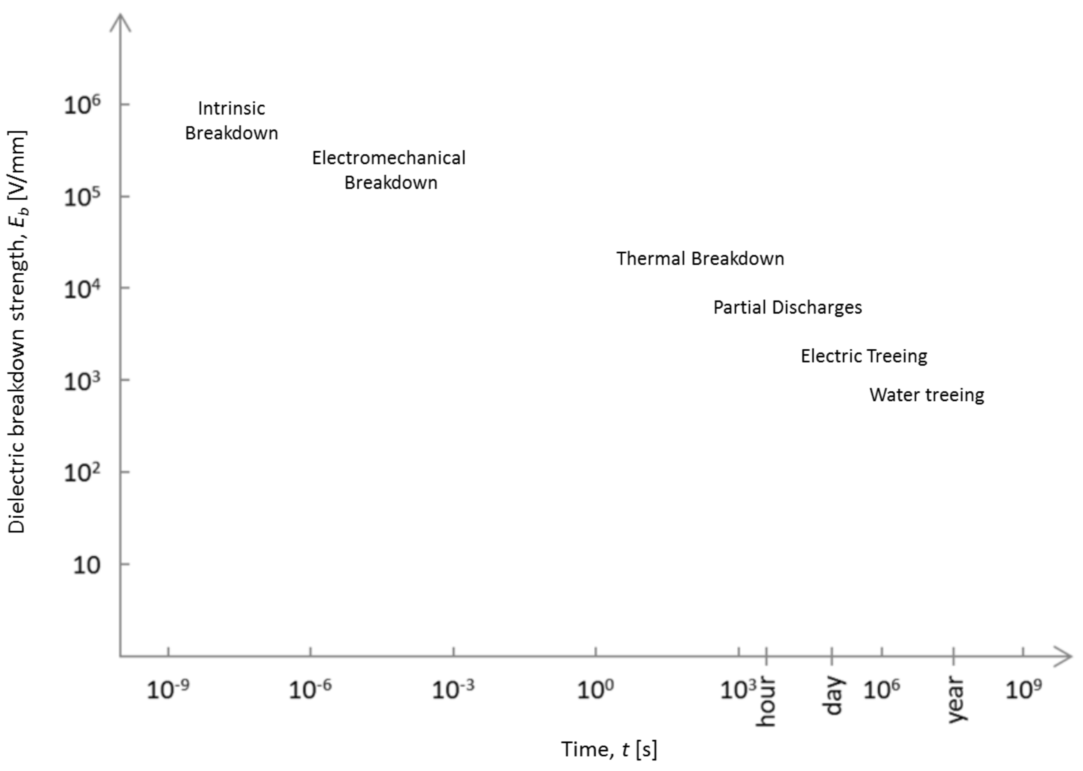

Figure 6. The variation of breakdown strength with time. Adapted from Aro et al. (2011) [5, 124].

Breakdown processes are also highly dependent on stress duration as the Figure 6 illustrates [5, 125].

3.1 Intrinsic Breakdown

The highest breakdown strength obtained is known as the "intrinsic strength" of the dielectric. Experimentally, this highest dielectric strength can be obtained only for very short time when all extraneous influences have been isolated and the value depends only on the structure of the material and the temperature. [5, 125; 6, 88]

3.2 Electromechanical Breakdown

In the electromechanical breakdown, the mechanical force between charges causes pressure which attracts the electrodes together and forces the dielectric to compress. As the dielectric compresses, the electrode distance decreases resulting the electric field to further increase pressure. Localized heating and softening of the dielectric caused by the pressure can lead to the mechanical collapse. The electromechanical breakdown is unlikely for typical insulators. [5, 125]

3.3 Thermal Breakdown

The thermal breakdown sets up the upper limit for improving the breakdown voltage by increasing the insulation thickness. In high-voltage systems thermal breakdown is common failure type and it occurs when heat is produced by electric field in the insulation faster than it is removed by cooling. [6, 90-91]

An insulator is never ideal. As a result of the charges moving through the insulator heat is produced. But in the presence of alternating electric field, the dielectric losses usually produce much more heat than the conductivity. Also the passage of an electric current through a conductor releases heat that is conducted to the insulation. [5, 127]

3.4 Partial Discharge

Discharges occur when critical field strength is exceeded locally. Partial discharge (PD) is localized electrical discharge that occurs between two conducting electrodes, without completely bridging the gap. It is a consequence of local electrical stress concentrations in the insulation or on the surface of the insulation. Partial discharges are often accompanied by the emission of heat, sound, light, and chemical reactions. [5, 125-126; 7, 15]

Partial discharges can be categorized into three groups: internal, surface and corona discharges. Internal and surface discharges can be extremely dangerous to the health of the insulation. Typically practical solutions where surface discharges occur are bushings and cable terminations. Corona is a form of partial discharge that occurs in gas around conductors which are remote from liquid or solid insulation. [5, 76; 6, 15]

3.4.1 Internal Partial Discharge

Internal PD occurs in defects of insulation. These defects can originate in a number of ways, for example because of manufacturing error, installation error, ageing and over stressing. Because of ageing, insulation naturally deteriorates and becomes less durable to the electrical stress. Over stressing and mechanical damages in-service can cause permanent damage to the insulation. Figure 7 illustrates defects that are exposed to internal PD. [5, 76; 8]

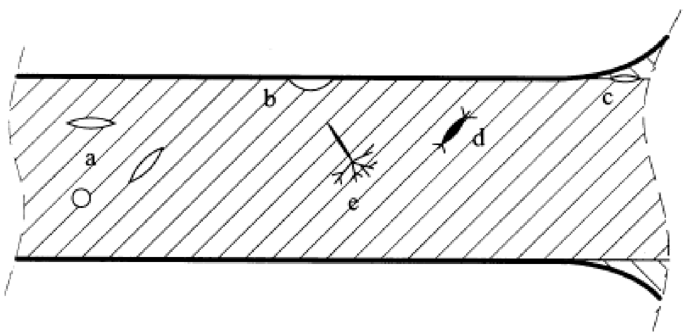

Figure 7. Defects that are exposed to internal partial discharge. a) Internal gas filled voids, b) void at the interface between insulation and electrode, c) void at the interface between insulation layers, d) foreign particles in insulation, e) already developed electric trees. Copied from Aro et al. (2011) [5, 76].

Often internal partial discharges occur in gas filled voids, because these voids usually have significantly lower dielectric strength than the surrounding material. If the void has lower permittivity than the surrounding dielectric, the voltage stress is also higher inside the void. Thereby under the normal electrical stress, the voltage across the void may exceed the breakdown value. The mechanism can be explained with the equivalent circuit, shown in Figure 8. [5, 77 & 126; 6, 99]

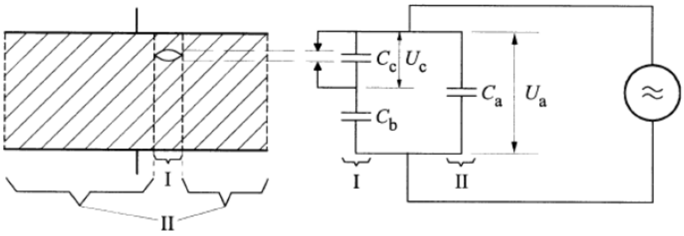

Figure 8. Equivalent circuit of dielectric with void. Copied from Aro et al. (2011) [5, 78].

In the equivalent circuit, C_c is the capacitance of the void, C_b is the capacitance of the dielectric which is in the series with the void, and C_a represents the capacitance of the rest of the dielectric. When the voltage U_c across the void reaches the breakdown voltage U_i (discharge inception voltage) of the medium in the void, discharge occurs and voltage over void collapses. When the voltage over the void drops below the discharge extinguishing voltage U_e, the discharge extinguishes and the voltage over the void builds up again till discharge occurs again. The number and frequency of the discharges will depend on the applied voltage U_a as Figure 9 illustrates. [5, 77-78; 6, 99-100]

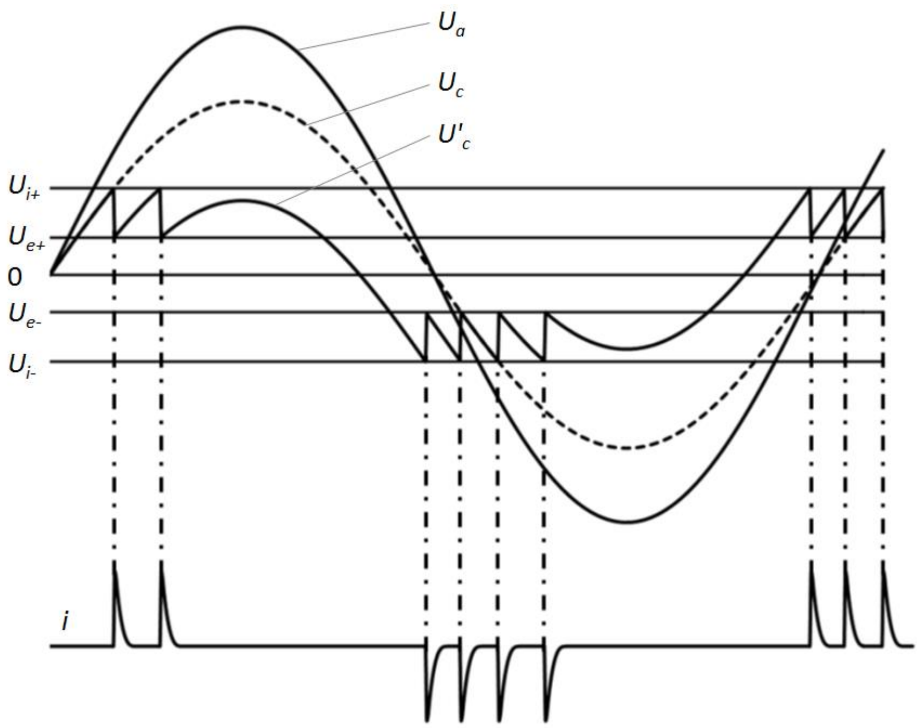

Figure 9. Voltage and current waveforms of internal partial discharges. Adapted from Aro et al. (2011) [5, 79].

In Figure 9 U_c describes the voltage across the void that would result from capacitance divider if no discharges occur and U'_c is the voltage across the void when the discharges occur. As the voltage and current waveforms of internal partial discharges illustrates, the discharges occur when the rate of voltage change is high. [5, 79-80]
Partial discharges can also occur with voltages below discharge inception voltage. When the discharge inception voltage is exceeded once (the voltage spike) and the discharge has occurred, discharges may continue depending on applied voltage, inception voltage and extinguishing voltage. The discharge inception voltages can also be unequal at negative and positive values, for example depending on the geometry of void. [5, 80-81]

When the discharges occur, the electrons and positive ions are formed. When the ions collide with the void wall, they may break the chemical bonds of insulation. Also in the each of the discharges, there will be heat dissipated in the voids which will cause the carbonization of the walls of void and erosion of the material. The gradual erosion of the material and consequent reduction in the thickness of the insulation can eventually lead to breakdown. This electrical breakdown can develop within a few hours up to several years. [5, 126; 6, 95-97]

3.5 Electrical Treeing and Water Treeing

Eventually discharges may advance through a solid insulator in a branching erosion path called electric tree. The electrical treeing is an electrical pre-breakdown phenomenon that weakens the dielectric strength of the material, enhances the electrical stress, and accelerates the PD process. [5, 126]

Another type of tree-like structure called the water tree can also form within polyethylene dielectrics. The water treeing begins at a microscopic inhomogeneous region and grows under the continued presence of electrical field and water. On the medium and high voltage cables, the water tree can eventually grow to the point where it bridges the outer ground layer to the conducting conductor, leading to the electrical breakdown. [5, 126 & 156]

4 Defining the Electric Field

As mentioned earlier, the breakdown of insulator is caused by energy provided by the electric field. When the effects of the defects in insulation are studied, it is essential to know how the electric field is divided inside insulating structures. The electric field in insulation can be defined with many different ways. The most of electric field calculations are nowadays done with numerical methods. With numerical methods two-dimensional and axially symmetrical electric fields can be solved with the great accuracy. On three-dimensional models somewhat inaccurate methods have to be used but the development in this area is strong. The field strength, the electric flux and the potential differences are calculated at each point of the examined area on the numerical method. Nowadays the finite element method (FEM) and the charge simulation method (CSM) are the most common numerical methods. [5, 31, 42 & 124]

The finite element method is originally used in the studies of the strength of materials but it can also be used to define different kind of fields. The basic idea of FEM is to divide a continuous structure into a finite number of sub regions (elements) as Figure 10 illustrates. [5, 42]

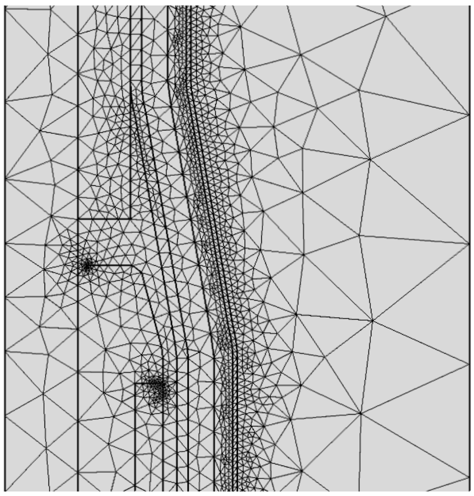

Figure 10. FEM mesh created by COMSOL Multiphysics.

The examined variable is potential in the electric fields. To minimize the calculation time, the field strength is assumed to be constant inside the element. This assumption can lead to the inaccurate results in highly inhomogeneous fields. The calculation accuracy can be easily increased by making the element net denser in the inhomogeneous area. [5, 44-47]

4.1 COMSOL Multiphysics

COMSOL Multiphysics is a simulation software which is based primarily on the finite element method. The software can be used for electrical, mechanical, fluid flow and chemical applications. With the add-on modules, the simulation platform can be expanded for modelling the specific application area. For example the AC/DC Module can be used for simulating the electric, magnetic, and electromagnetic fields in low-frequency and static applications. There are also the add-ons for interfacing with the third-party software, for example the CAD Import Module. [9]

5 Medium Voltage Underground Cables

The medium voltage is imprecise voltage range that is not defined by the standards. Nowadays the underground cables are commonly plastic insulated. A Harmonization Document HD 620 is a normative document made by CENELEC and it applies to the cables with the extruded insulation and for the rated voltages U_0/U (U_m) from 3.6/6 (7.2) kV up to and including 20.8/36 (42) kV. In the underground cable industry this voltage range is often described as the medium voltage. The U_0 in the rated voltages is the RMS value between any phase conductor and earth, U is the RMS value between any two phase conductors and U_m is the maximum RMS value of the highest system voltage where the equipment can be used. [10, 303; 11, 3-5]

5.1 The Structure

The medium voltage cables usually consist of the following components: the conductor, the conductor screen, the insulation, the insulation screen, the shield and the outer sheath. [10, 307]

The conductor is usually made of aluminum or copper. Aluminum is the most common conductor material, because it is cheaper and lighter than other metals. Copper is used in some cases, because it has better conductivity than aluminum. Conductors are usually circular and made of stranded wires. Stranded conductors are used, because they are more flexible than solid conductors. Circular shape is used to minimize the electric field strength on the surface of the conductor and the risk of partial discharges. For same reason conductors are often compacted. [10, 307-308]

The conductor is covered with a semiconducting *conductor screen*. The conductor screen is used because the insulation cannot be attached airtightly to the conductor. When the semiconducting conductor screen is tightly attached to the insulation, there is no air voids at the interface of the insulation and the electrode. So the conductor screen provides a smooth surface on the same potential as the conductor to keep electric field consistent. In fault situations the screen also reduces thermal stress of the insulation. Generally conductor screens are required for polyethylene insulations above 3.6/6 (7.2) kV. With polyvinyl chloride insulation the screen is required with rated voltages above 5.8/10 (12) kV. [10, 308]

The insulation isolates the conductors from each other and from the insulation screen and the shield which are at the ground potential. The purpose of the insulation is to provide enough dielectric strength and sufficiently transfer the generated heat out from the cable. The different types of plastics are nowadays common insulation materials but also the oil impregnated papers and rubbers are used as the insulation. [10, 308]

The insulation is covered with *the insulation screen*. The Insulation screen is made of conducting metal or semiconducting material and it has similar function to the conductor screen. The screen provides a smooth transition from the insulation to the grounded shield. [10, 310]

The conducting metal *shield* on top of the insulation screen acts as a second electrode of the capacitor formed by the cable. The shield nullifies the electric field outside of the cable and also functions as a return path for ground-fault currents. Also the mechanical protection is provided by the shield. The shield can be either individual for each phase or shared with all the phases. The usual shield materials are aluminum, copper and lead. [10, 310]

The final layer of the cable is *the outer sheath* which provides mechanical protection and protection from corrosion. The outer sheath can be made of plastic, rubber or metal. [10, 311]

5.2 AHXCMK-WTC

AHXCMK-WTC is a medium voltage cable for fixed installation indoors and outdoors. This cable type is manufactured at two voltage levels which are 6/10 (12) kV and 12/20 (24) kV. There is 1-core and 3-core version of the cable. In 3-core version the metal shield is shared with all phases. [12]

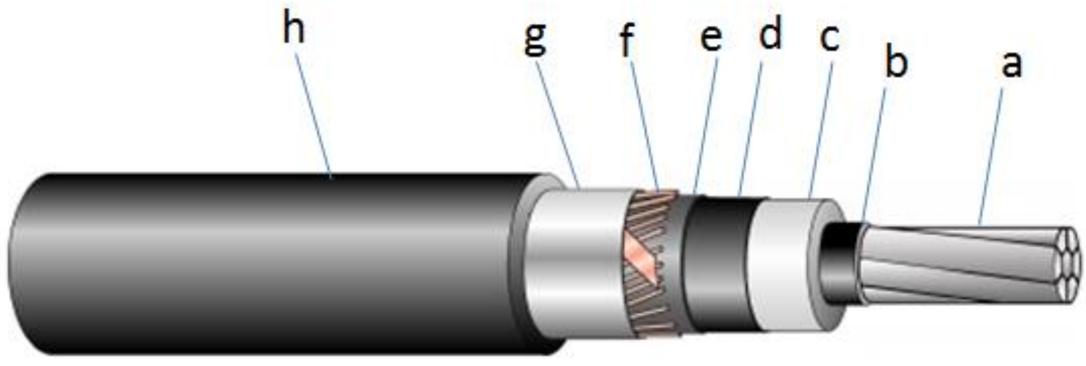

Figure 11. 1-core medium voltage cable AHXCMK-WTC. Copied from Reka Cables Ltd. (2015) [13].

1-core AHXCMK-WTC cable construction (Figure 11) [12]:

a) Conductor, longitudinally watertight stranded aluminum
b) Conductor screen, semiconductive cross-linked polyethylene
c) Insulation, cross-linked polyethylene (XLPE)
d) Insulation screen, semiconductive cross-linked polyethylene
e) Semiconducting waterswellable tape against longitudinal water penetration
f) Shield, layer of copper wires with a copper tape
g) Binder tape
h) Outer sheath, polyvinyl chloride (PVC)

The cable used in the testing was Reka's 1-core 150 mm^2 AHXCMK-WTC 12/20 (24) kV. A simplified structure of AHXCMK-WTC was used in the simulation. This cable type was chosen because it has outer sheath made of PVC, which is easy to cut and remove. Copper wire shield makes also the installation easier and faster compared to other types of shields.

6 Medium Voltage Underground Cable Joints

The cable joint is an accessory which makes the connection between two or more insulated power cables to form a continuous circuit. Straight joint is accessory used for making a connection between two cables. Branch joint is used to make a connection of branch cable to a main cable. Cable accessories are the weakest points in the distribution line because they are more defect-prone than cables. These defects exist due to poor installation, in-service or manufacturing process. The aim of the jointer and manufacturer is to obtain a joint whose properties are as good as the original cable in both electrical and mechanical terms. [14, 6; 15, 1051]

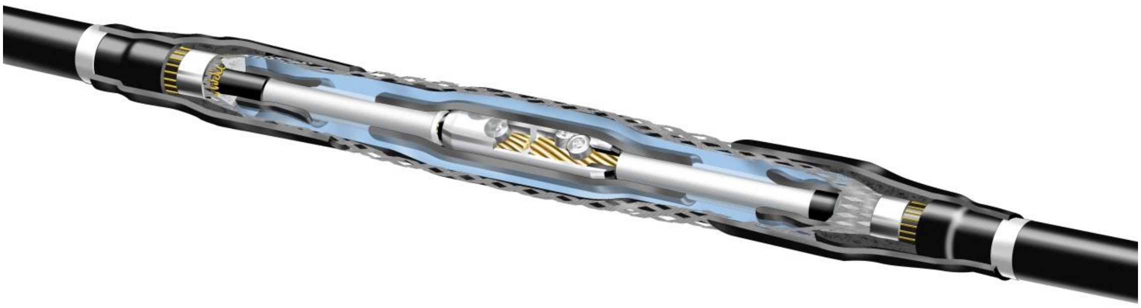

Figure 12. Cold shrink medium voltage cable joint. Copied from Ensto Group (2015) [16].

The structure of joint (Figure 12) depends on the cable type, used voltage and operating environment. Medium voltage joint structure is somehow similar to a cable structure and usually includes connector, stress control, joint insulation, joint insulation screen, joint shield and outer sheath. [10, 330-331; 17]

The conductors are connected with *a connector* that can be pressed, welded or mounted by screws. To prevent the electric field peaks, the connector surface must be cylindrical and smooth. The surface can be smoothened by adding a semiconducting tape on top of the connector. [10, 330-331]

The installation of cable joint requires the removal of the insulation screen from the end of the cable. The problem in jointing is that the electric field rises remarkably at the cut edge of the insulation screen as Figure 13 illustrates. [17; 18, 47]

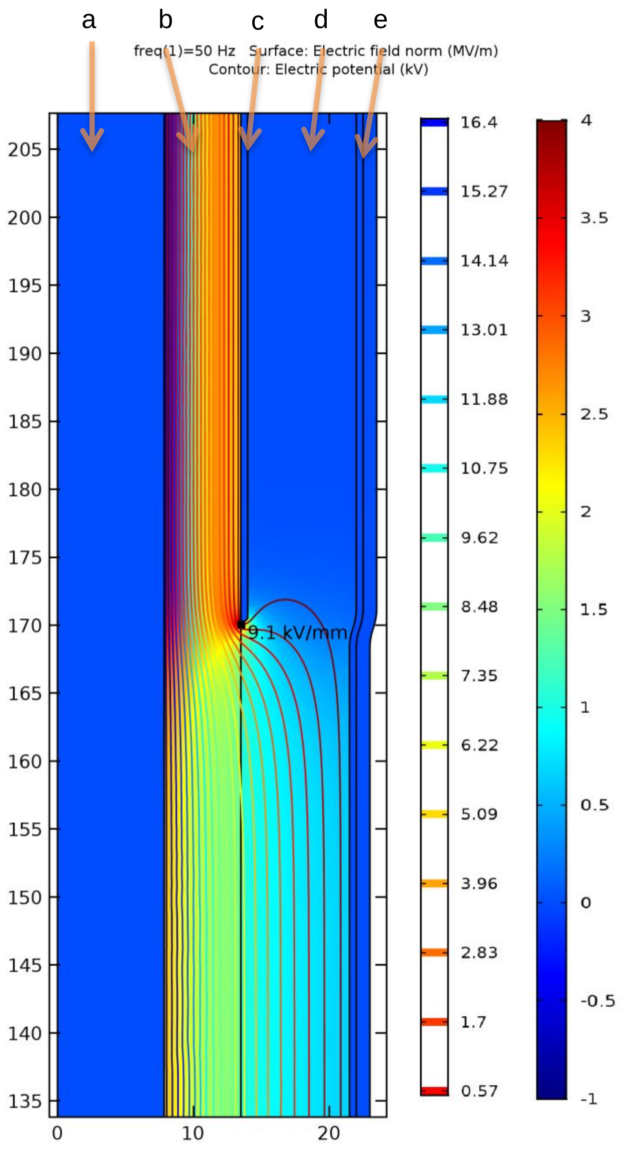

Figure 13. Electric stress distribution inside a cable joint without stress control. a) conductor b) cable insulation c) insulation screen d) joint insulation e) joint insulation screen.

Figure 13 shows the simulation of electric stress distribution inside a cable joint without stress control at the cut-off point of the insulation screen. The color scale of surface plot illustrates electric field strength and electrical potential is displayed with equipotential lines. In this simulation the electric potential of conductor is 12 kV (50 Hz). The electric field is concentrated at the cut edge of insulation screen and in this case the peak value calculated is 9.1 kV/mm. This stress would be high enough to ionize the air causing discharges. Because it is hard to make the interface between joint insulation, cable insulation and insulation screen air tight, some sort of *stress control* is required. Also with higher potential or voltage spikes even the critical breakdown strength of the insulating material can be achieved.

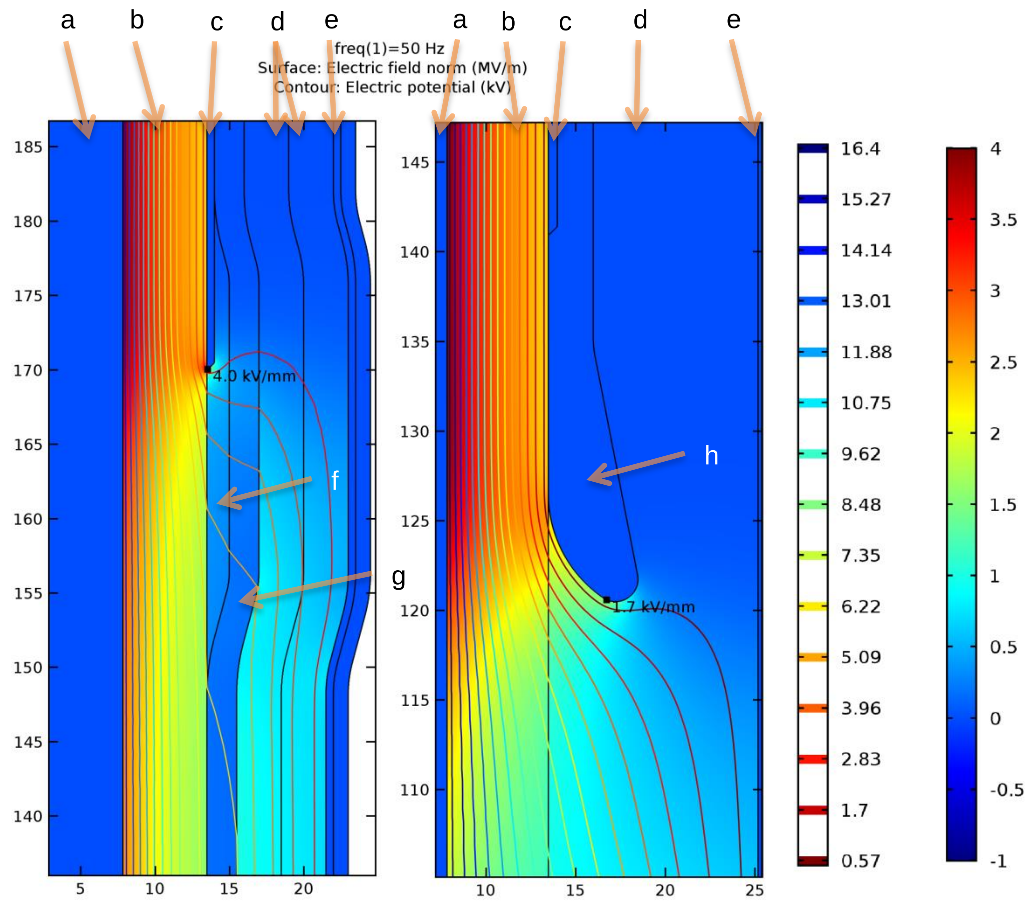

Figure 14. Electric stress distribution with refractive stress control (left) and geometrical stress control (right). Components: a) conductor b) cable insulation c) insulation screen d) joint insulation e) joint insulation screen f) stress control mastic g) stress control tube h) stress control cone.

Figure 14 illustrates simulations from two common types of stress control alternatives. The left one is called a refractive stress control and the right one is called a geometrical stress control.

The main idea of the refractive stress control is to use an additional insulating layer with the high permittivity. In this case two layers are used. High permittivity *stress control tape* (f) is first wrapped around the area with a high electrical stress. This stress control mastic also reduces significantly the possibility of air voids in the critical area. The second layer used is *stress control tube* (g). The permittivity of the stress control tube is much higher than the permittivity of the insulation. As the result of the high permittivity, the electric field concentration at the cut edge of the insulation screen spreads more evenly. The peak value of the electric field strength is reduced in this example to 4.0 kV/mm. [17; 18, 50]

The main idea of the geometrical stress control is to reduce the electric field strength by adding *a cone shaped conductive electrode* (h) on top of the cable at the cut edge of the screen. The electric field distributes thereby more evenly. In this example the value of electric field strength in the end of the stress control cone is only 1.7 kV/mm. [17; 18, 48]

The insulation material of the joint depends on the used cable type. Materials like plastics, tapes, paper ribbons, cable mass and cable oil can be used. The purpose of the joint insulation is to provide enough dielectric strength and to sufficiently transfer the generated heat out from the joint. [10, 330; 17]

The insulation screen of the joint can be implemented with semiconducting materials. The purpose of the screen is to provide a smooth transition from the joint insulation to the grounded joint shield. [10, 330; 17]

The conducting shields of the cables are connected with *a joint shield* that has similar function as cable shield. For example the joint shield can be made of copper gauze. [10, 330; 17]

Finally the joint is covered with *the outer sheath* which protects the joint from mechanical stress. The outer sheath is usually made of plastic or metal depending on the surrounding environment. [10, 330]

Cable joints can be categorized into different groups by dividing them based on the used installation technology. The most common used applications in medium voltage joints with extruded cables are heat shrink and cold shrink technologies and combinations of these two. [19, 410-416]

6.1 Heat Shrink Joints

In the heat shrink technology polymeric materials are used. The heat shrinkable property is imparted by first molding or extruding the polymeric material into the required shape and then subjected to crosslinking by a radiation beam or by chemical means. After crosslinking, the component is warmed and expanded and then allowed to cool in this expanded state. When the heat is applied again during installation, the component tries to return back to the shape which it had during crosslinking process. The early versions of medium voltage heat shrink joints consisted of a number of tubes to provide stress control, insulation, screening and outer sheath. Nowadays designs combine these layers, for example by combining the insulation and screening as a single co-extrusion, making installation faster and easier. [19, 412]

6.1.1 HJ11.2403C

The heat shrink cable joint examined in this thesis was the HJ11.2403C (Figure 15).

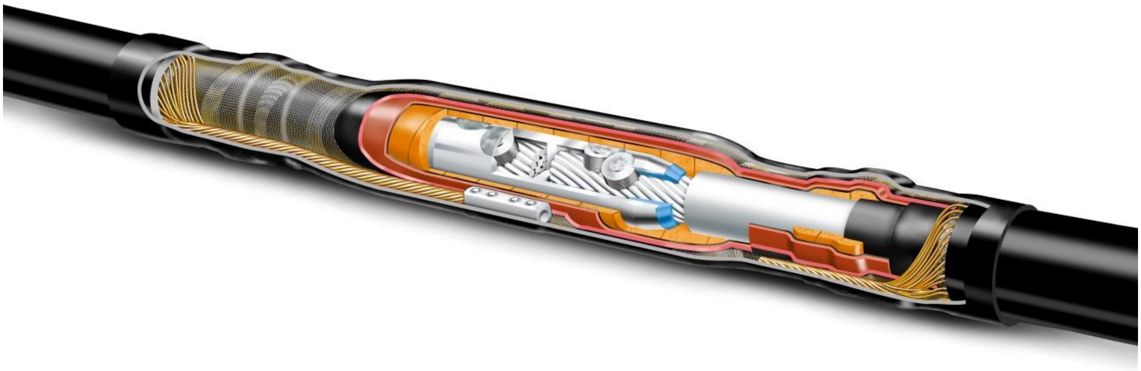

Figure 15. HJ11.2403C. Copied from Ensto Group (2015) [16].

The kit is suitable for jointing of maximum 12/20 (24) kV single core cables with XLPE insulation and copper wire shield. The conductor range for this product is 70 – 240 mm^2. [20]

Figure 16. HJ11.2403C heat shrink joint kit. Adapted from HJ11.2403C Product Card (2015) [20].

HJ11.2403C heat shrink joint kit (Figure 16) includes following materials [20]:

a) Sealing tube CPEEPL (outer sheath)
b) Insulating and semiconductive tube SIST (insulation and insulation screen)
c) Stress control and insulating tube SISCT (stress control and insulation)
d) Sealing mastic SSM75 (waterproofing)
e) Stress control tape SSCTA85 (void filling and stress control)
f) Grinding paper
g) Tinned copper tape (joint shield)
h) Medium voltage shear head bolt connector SMJ2.47 suitable for aluminum and copper conductors
i) Low voltage shear head bolt connector SLJ1.47 for connecting shield wire
j) Grey mastic for filling screw holes
k) Cleaning tissues
l) PVC tape
m) Peeling rope

6.2 Cold Shrink Joints

The elastomeric materials are used in the cold shrink technology. There are two basic types of the cold shrinks, stretch rubber type and pre-stretched type which is expanded in the factory on to a plastic support tube. Like the heat shrinks, the cold shrink products can accommodate a wide range of cable diameters, but they offer a number of advantages. Gas bottles and torches are unnecessary during installation and the quality of assembly is less dependent upon the skill of the installer. The cold shrink products usually have fewer separate components, which makes the installation faster and easier. In addition, the elastomeric cold shrink continues to shrink towards its original shape after the installation unlike the heat shrink, which "freezes". Therefore the cold shrink is capable of following any subsequent movement. [19, 414]

The elastomeric materials that are used in the cold shrinks are not as strong against environmental stress as materials used in the heat shrinks. For this reason so called hybrid joints are used. The hybrid joint is a mix of heat shrink and cold shrink products. The price can also be reason for combining the technologies. Often in the hybrid joints the outer sheath is made of the heat shrink tube. In this way electrical properties are similar to the total cold shrink product but the mechanical strength is increased. [17]

6.2.1 CJH11.2403C

The cold shrink cable joint examined in this thesis was CJH11.2403C that is actually a hybrid joint with a heat shrink outer sheath. The kit is suitable for jointing of maximum 12/20 (24) kV single core cables with XLPE insulation and copper wire shield. The conductor range for this product is 70 – 240 mm^2. [21]

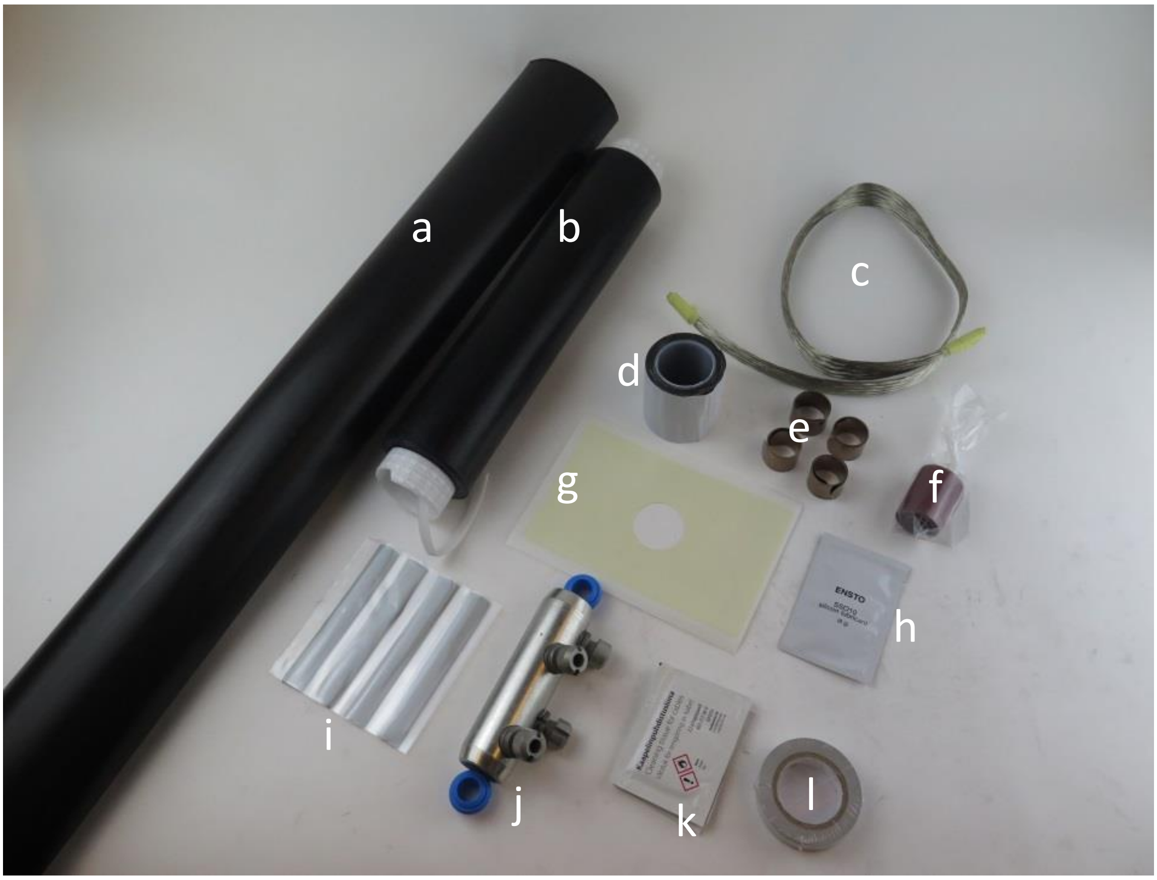

Figure 17. CJH11.2403C hybrid joint kit.

CJH11.2403C hybrid joint kit (Figure 17) includes following materials [21]:

a) Sealing tube CPEEPL (outer sheath)
b) Cold shrink joint body (stress control, insulation and insulation screen)
c) Tubular copper net (joint shield)
d) Self-amalgamating tape SSATA10 (waterproofing)
e) Constant force springs for connecting shield wires to tubular copper net
f) Grinding paper
g) Adhesive protection sheet for smoothening the connector surface
h) Silicone lubricant
i) Grey mastic for filling the space between the outer sheath of the cable and the joint body
j) Medium voltage shear head bolt connector SMJ2.47 suitable for aluminum and copper conductors
k) Cleaning tissues
l) PVC tape

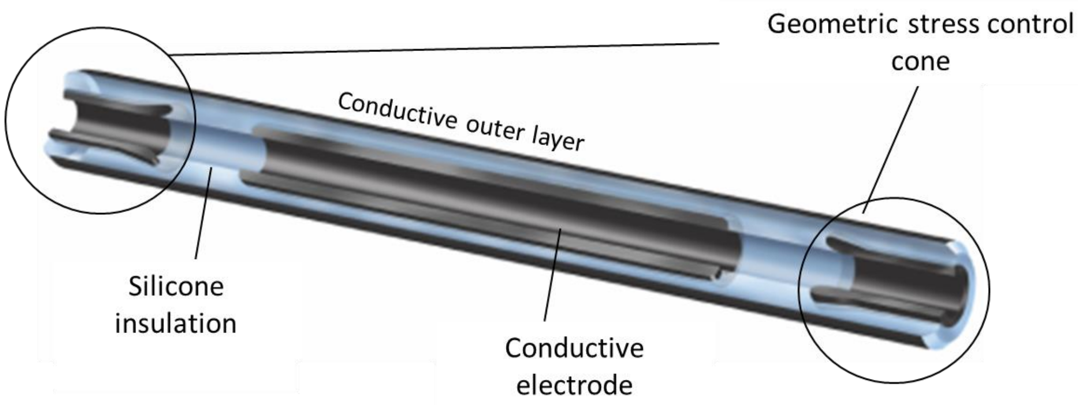

Figure 18. Sectional view of cold shrink joint body. Copied from Ensto Pro Training Academy material: Solutions for Underground Cable Networks (2015) [17].

Figure 18 illustrates section of the cold shrink joint body. The joint body includes insulation, stress control and the insulation screen. This makes the joint less vulnerable to installation errors and also the installation is faster and easier compared to the heat shrink products.

7 Electric Field Simulation

A total of six electric field simulations were made in this thesis. Two common fault types were studied on both heat shrink and cold shrink joint. Also a reference simulation was made on both joint types. The fault types were:

1. Irregularities on the surface of the cable insulation caused by faulty shaving of the cable screen (both joint types)
2. Air between the heat shrink tubes
3. Faulty positioning of the cold shrink joint body

The simulations were done with 2D axial symmetric models as shown in Figure 19a. The models were generated with AutoCAD software according to sample joints and installation instructions that can be found in Appendices 1 & 2. The joints were assumed to be axial symmetrical and the screw holes and the screws were left out from simulations. Also all simulated defects were axial symmetrical. The models are drawn from the center of the conductor outwards to the right side of the joint.

Some simplifying is done in models because they do not have effect on simulation. Conductor and conductor screen are modelled as one solid aluminum part. The outer sheath of joint and the waterproofing are also left out of model, because they do not have effect on electric field simulation.

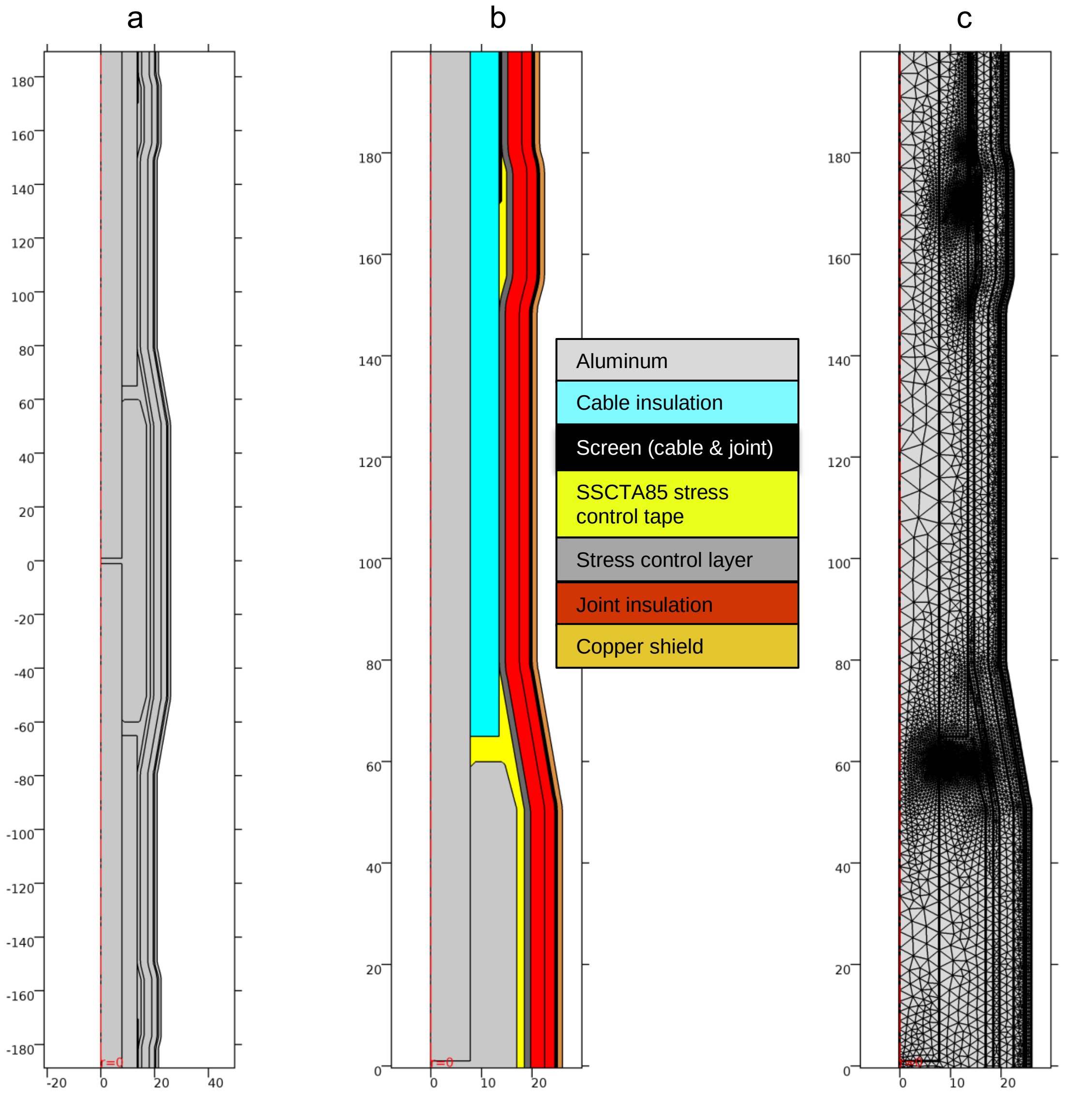

Figure 19. a) 2D model of axial symmetric HJ11.2403C joint without installation defects, b) material properties applied to model, c) meshed model.

After importing the model, the electric properties of all the domains were specified. The values used in the simulations are listed in Table 1.

Table 1. Electric properties used in simulation.

Material	**Electrical conductivity, σ (S/m)**	**Relative permittivity, ε_r**
Air	3×10^{-15} [22]	1 [23]
Aluminum (conductor and connector)	$3.774\text{x}10^{7}$ [23]	-
Copper (shield)	$5.998\ \text{x}10^{7}$ [23]	-
XLPE (cable insulation)	$1\text{x}10^{-14}$ [24]	2.25 [25]
Insulation screen	1 [26]	-
Stress control tape SSCTA85	$1.4\text{x}10^{-8}$ [27]	11 [27]
Stress control tube SISCT, inner layer	$1\text{x}10^{-11}$ [27]	22 [27]
Stress control tube SISCT, outer layer	$3.9\text{x}10^{-15}$ [27]	3 [27]
Insulating and semiconductive tube SIST, inner layer	$3.9\text{x}10^{-15}$ [27]	3 [27]
Insulating and semiconductive tube SIST, outer layer	0.001 [28]	-
Cold shrink joint body, insulation	$1\text{x}10^{-16}$ [27]	2.75 [27]
Cold shrink joint body, stress cones and outer layer	2.22 [29]	-

After applying the material properties, the conductor was set as a voltage terminal and the copper shield of the cable as a ground. A voltage of 12 kV and 50 Hz was used in the simulations. Next thing to do was to generate the finite element mesh for the model as shown in Figure 19c. The simulation can be solved after the finite element mesh is generated.

The magnitudes of the electric field peaks are the points of interests in the simulations. The simulations are studied at the moment of peak voltage when the electric field strength is also at the highest point. The field peak values are compared to dielectric strength values of insulating materials. As mentioned earlier, the discharges occur when the critical field strength is exceeded locally. The dielectric strengths of insulating materials are listed in Table 2.

Table 2. Dielectric strengths of insulating materials.

Material	**Dielectric strength, E_{max} (kV/mm)**
Air	3.0 [2, 17]
Cable insulation (XLPE)	~35
Stress control tape SSCTA85	~11
Stress control tube SISCT, outer layer	>25 [28]
Insulating and semiconductive tube SIST, inner layer	>25 [28]
Cold shrink joint body, insulation	>40 [29]

High voltage test was used to determine the dielectric strength of the cable insulation and the stress control tape. On the test, the test sample was placed between two electrodes, which were submerged in transformer oil inside a glass bowl. The voltage was generated by a high voltage AC transformer that was connected to one of the electrodes. The other electrode was connected to the ground. The voltage was increased by 500 V/s until breakthrough of the test sample occurred and the dielectric strength of the sample was then calculated.

7.1 Reference Heat Shrink Joint

The cutting points of the cable screenings and the surface of connector are the points of interests in the HJ11.24 heat shrink joint as Figure 20 shows.

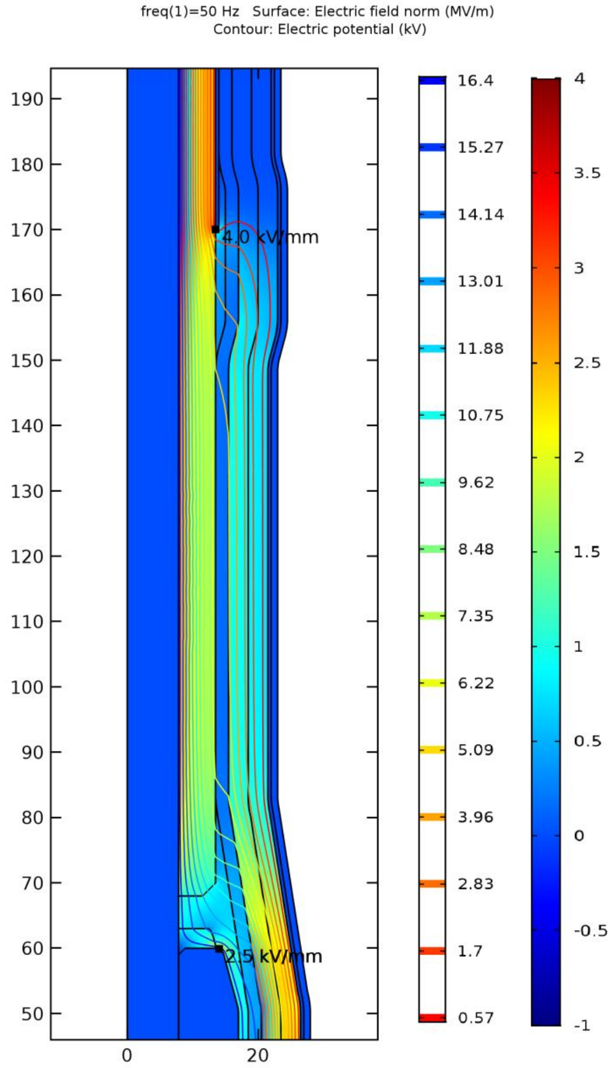

Figure 20. Simulation of the HJ11.2403C joint without installation-based defects.

The color scale of the surface plot illustrates electric field strength and the electrical potential is displayed with the equipotential lines. The electric field peak at the interface between stress control tape and the connector is 2.5 kV/mm. At the interface between the cable screen, the stress control tape and the cable insulation, the field strength is 4.0 kV/mm. These peaks are not crucial because the dielectric strength of stress control mastic is about 11 kV/mm. According to the simulation, the dielectric strength of the mastic is reached at the cut edge of the screen when the voltage U_0 is 33 kV.

7.2 Reference Cold Shrink Joint

The electric field peaks are generated at the interfaces between joint electrodes and insulating joint body in the CJH11.24 cold shrink joint as Figure 21.

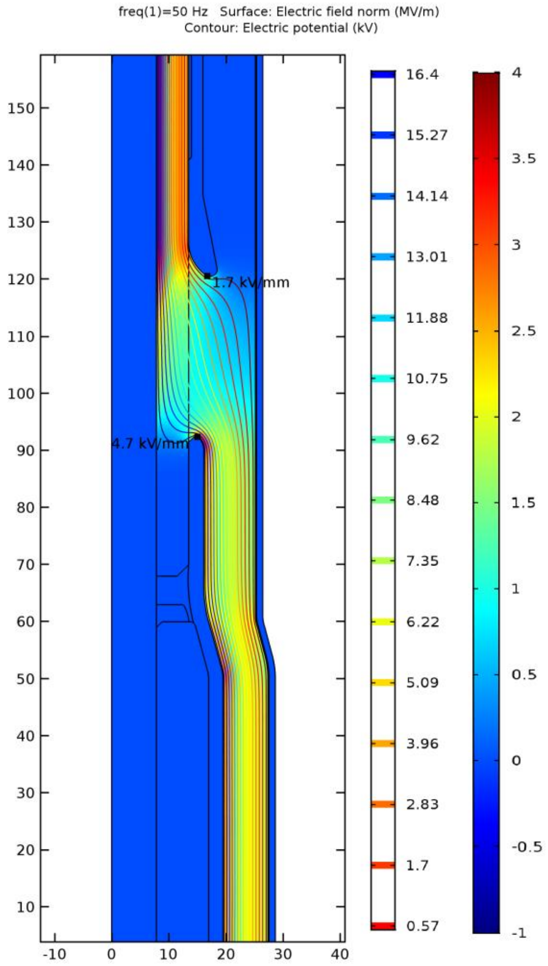

Figure 21. Simulation of the CJH11.2403C joint without installation-based defects.

The electric field strength in the end of stress control cone is 1.7 kV/mm and at the interface between the conductive connector electrode and the joint insulation the peak value is 4.7 kV/mm. These electric field peaks are not crucial because the dielectric strength of the insulation of the cold shrink joint body is above 40 kV/mm. According to the simulation the dielectric strength of the joint insulation is reached on the surface of the connector electrode when U_0 is over 102 kV. The discharges would likely occur with lower voltage in the microscopic air voids, which are left on the interface of the joint body and the cable insulation in the real joints.

7.3 Fault Type 1: Irregularities on the Surface of the Cable Insulation

The removal of the insulation screen from the end of the cable is one of the most crucial stages of the joint installation. There are different kinds of shaving tools which are designed to remove the bonded semiconductive screen. Some irregularities will be left on the cable insulation after the shaving. These irregularities should be smoothened with the grinding paper but sometimes the assemblers have been found to skip this grinding even if the surface of the cable insulation is highly uneven as shown in Figure 22.

Figure 22. The shaving marks found from a cable joint that was removed from the distribution network.

If the surface of insulation is uneven enough, some air cavities will be left between the insulation and the shrinking tube. In this work, the irregularities on the surface of the cable insulation were imitated by shaving three 1 mm deep grooves with shaving tool as Figure 23 shows.

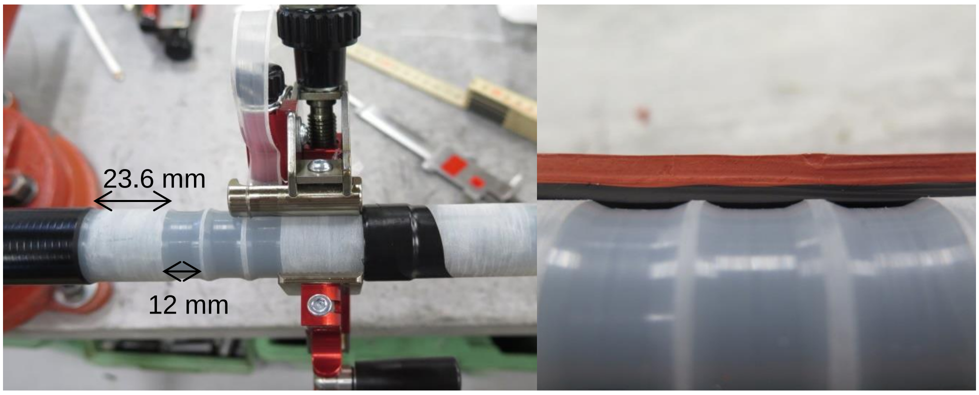

Figure 23. The making of the irregularities (left). The heat shrink joint which has been cut open shows the air cavities left inside the joint (right).

The distance between each groove was approximately 1 mm. The Figure 23 also shows an opened sample that was used as a help for modeling the cavities in the simulation.

7.3.1 Heat Shrink Joint

Figure 24 shows simulation results of the HJ11.2403C joint with the irregularities on the surface of the cable insulation.

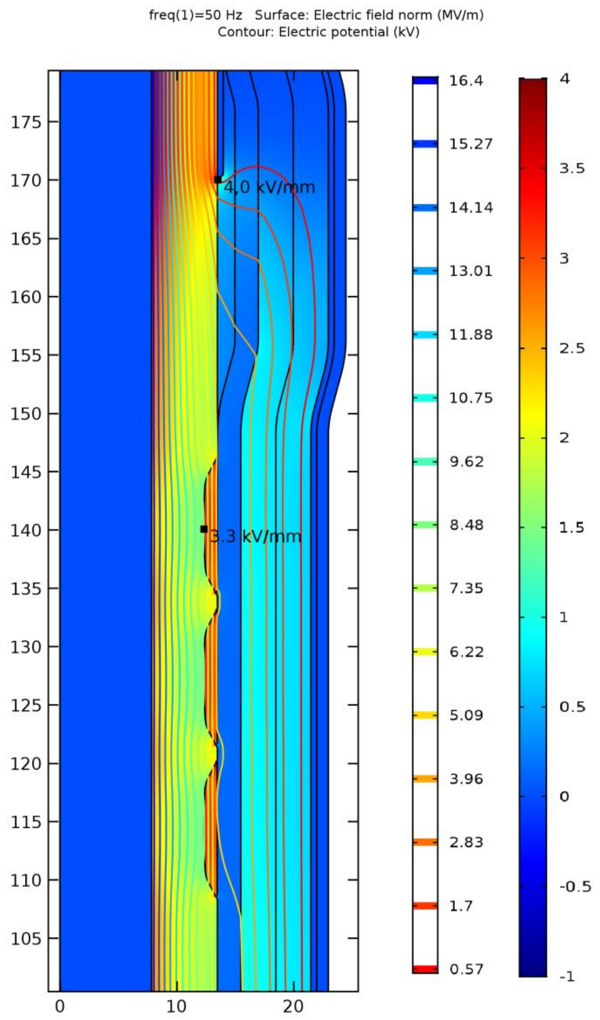

Figure 24. Simulation of the HJ11.2403C joint with the irregularities on the surface of the cable insulation.

The results show that the electric field concentrations with the magnitude of 3.3 kV/mm were generated at the air voids. According to the simulation, the dielectric strength of the air (3.0 kV/mm) is reached in these cavities when phase to neutral voltage is 11 kV.

7.3.2 Cold Shrink Joint

Because the cold shrink joint body is elastomeric, the study of cavities between the insulation and the joint body was not as simple as with the heat shrink joint. When the sample of the cold shrink joint was cut open, tension of the joint body dropped. It seemed like that no air voids were left between the joint body and the insulation in this case. Since the behavior of the joint body was not completely clear, the simulations with and without air voids were made.

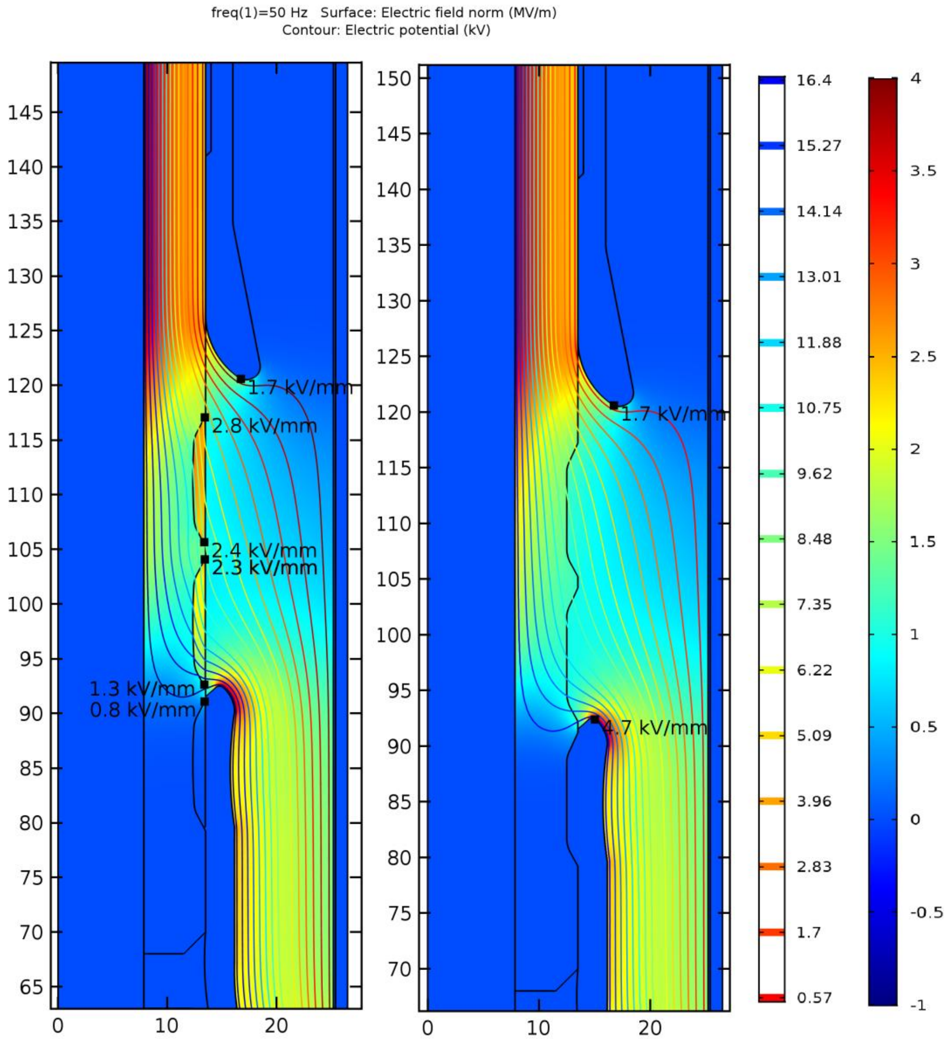

Figure 25. Simulations of the CJH11.2403C joint with the irregularities on the surface of the cable insulation. Left one with the air voids and right one without the air voids.

As the Figure 25 illustrates without the air voids, the electric field distribution was almost identical to the reference model. With the air voids, the higher electric field concentrations are generated at the air voids. The magnitude of the field strength varies highly based on the location. According to the simulation, the highest peak value in the air cavities was 2.8 kV/mm. The electric stress at this point reaches the dielectric strength of the air when U_0 is 13 kV. In the void which is under the connector electrode, the critical field strength is achieved when the voltage U_0 is 45 kV.

7.4 Fault Type 2: Air between the Heat Shrink Tubes

The shrinking of the heat shrink tubes is crucial part in the cable jointing. It is essential to follow the installation instructions to avoid trapped air under the tube in the shrinking. Figure 26 shows an opened cable joint that was removed from the network after 5 months use because the noise was heard from it. In this joint, the white marks are caused by discharges that were result of trapped air between the tubes. [30]

Figure 26. Discharge marks caused by trapped air between the tubes. Copied from Alkila (2015) [30].

This fault type was imitated by grinding three 1 mm deep grooves on top of the stress control and insulating tube in this work as shown in Figure 27. One joint with this type of air voids was made, opened and used as a help for the modeling.

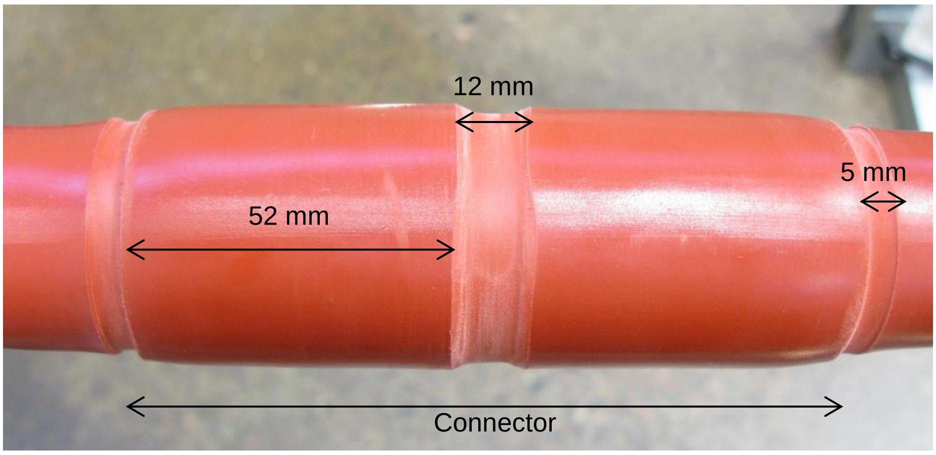

Figure 27. Grinded surface of the stress control and insulating tube.

Figure 28 shows the simulation result of the heat shrink joint with air voids between the heat shrink tubes.

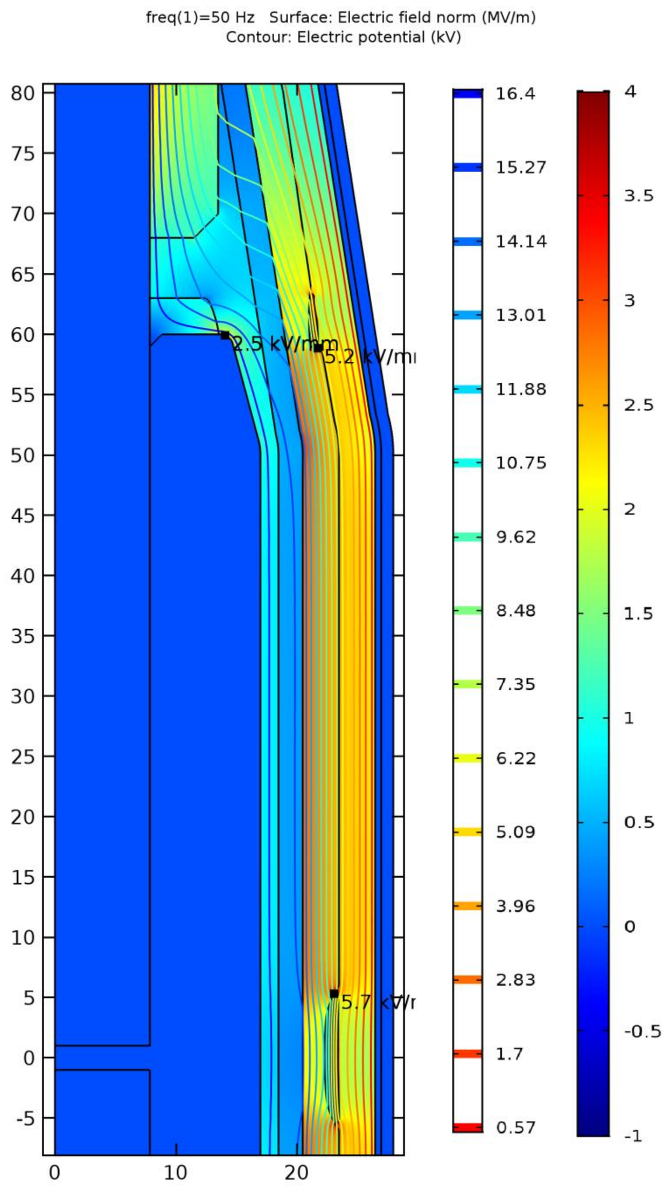

Figure 28.Simulation of the HJ11.2403C joint with air voids between the heat shrink tubes.

The results show that the high electric field concentrations were generated at the air voids. The highest magnitude recorded in the simulation was 5.7 kV/mm. According to the simulation, the dielectric strength of the air at this point is reached when U_0 is over 6 kV. In the air void which is on top of the corner of the connector, the dielectric strength of the air is reached with the phase-to-neutral voltage of 7 kV.

7.5 Fault type 3: Faulty Positioning of the Cold Shrink Joint Body

The positioning is a crucial part of the installation of the cold shrink because the electric field distribution can be disturbed significantly if the insulation screens are not covered with the stress control cones. The purpose was to study a situation where the cut edge of the insulation screen is between the stress control cone and the connector electrode. This positioning error was decided to be imitated by changing the shaving length of the cable insulation screen on the other cable.

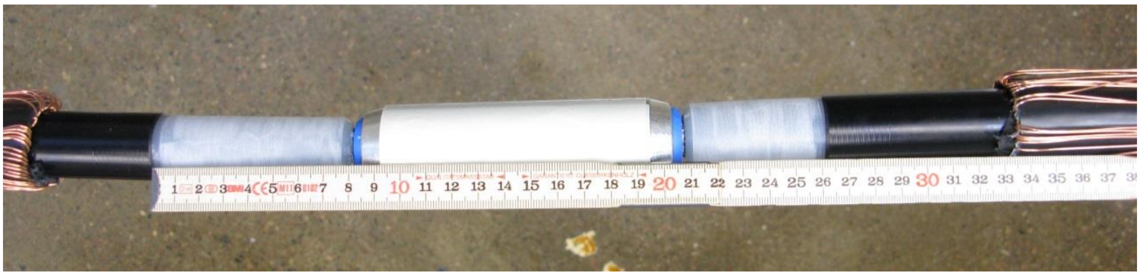

Figure 29. Too short insulation screen shaving on the right side of the connector.

As the Figure 29 shows the removal of the insulation screen was 25 mm too short on the other cable and on the other cable the screen was removed according to installation instructions in studied joints. Because the cold shrink joint body is able to follow the shapes of the cable surface well, it was assumed that no air voids were left at the cut edge of the screen.

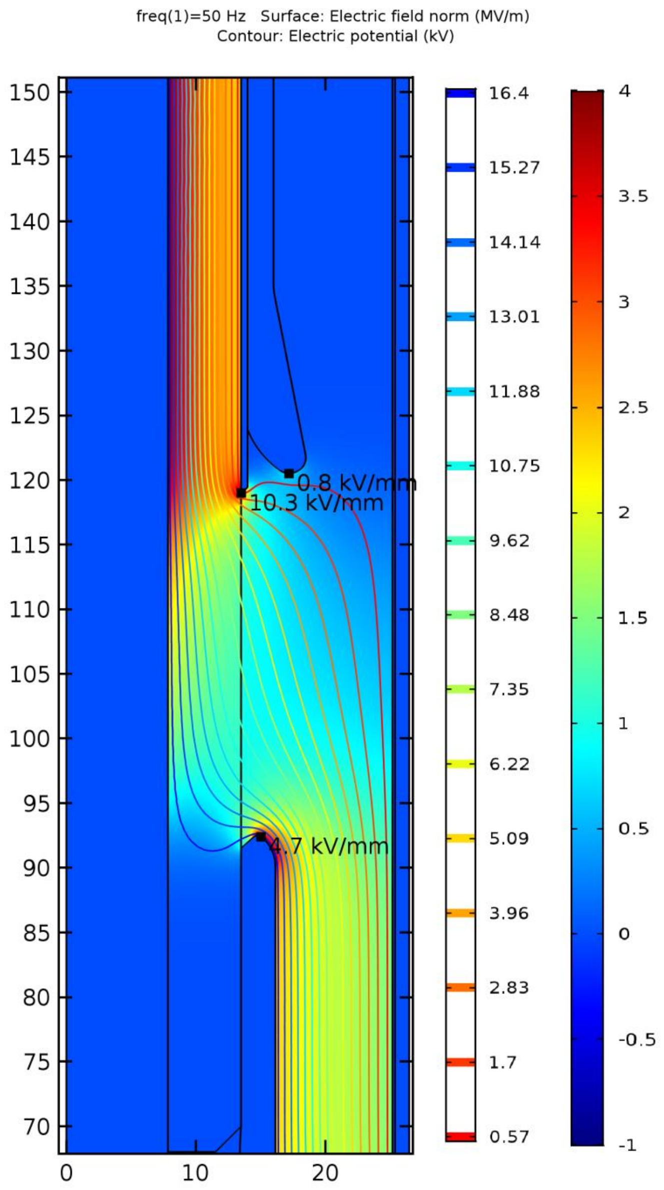

Figure 30. Simulations of the CJH11.2403C joint with too long insulation screen.

As the Figure 30 illustrates the stress control is almost completely inactive in this case. The highest electric field peak is generated at the cut edge of the insulation screen. The magnitude of this peak is 10.3 kV/mm. However, because the dielectric strengths of the cable insulation and the joint insulation are fairly high, this electric stress is not enough to cause the discharges. The dielectric strength of the cable insulation is reached at the cut edge when the voltage U_0 is 41 kV according to the simulation.

8 Electrical Testing

The verification of the simulation results were done by studying the partial discharge inception voltages (PDIV) with the partial discharge test. The PD test results were also used as a help to determinate the seriousness of the installation errors. The behavior of the joints was also studied with the AC voltage step test. Only the joints with the installation-based defects were tested to save time. Also Ensto already had enough information about the behavior of both studied joint types without installation-based defects.

Both joints which have been studied are type tested according to the CENELEC's harmonization document HD629.1 that defines the general test requirements for the medium voltage accessories used on the extruded cables. For example this document requires that during the partial discharge test at the ambient temperature maximum discharge level allowed at two times U_0 is 10 pC. The AC voltage dry test is also one of the tests required by HD629.1. This test requires that the joint is able to withstand the AC voltage of 4.5 times U_0 for 5 minutes without the breakdown. [14, 18]

8.1 Testing Procedure

12 cable lines were prepared for the test. Ensto's CIT1.2403L terminations were installed to the cables and the partial discharge measurements were performed to all the lines in order to verify the quality of the installation. All the lines were free of the discharges at 40 kV. After this, the joints with the defects were installed to the test lines. Three samples of each fault types were tested. First the partial discharge inception voltages were measured and after that the AC voltage step test was performed. Each cable line was tested separately.

8.1.1 Partial Discharge Test

Before each partial discharge test, the measurement instrument was calibrated using a charge calibrator. After the calibration the background noise was recorded at the minimum voltage level. The voltage was then increased slowly up to 40 kV or until the discharge level was too high. The determination of the partial discharge inception and the extension voltages were the main focuses of the test, but also the discharge levels were recorded at the certain points.

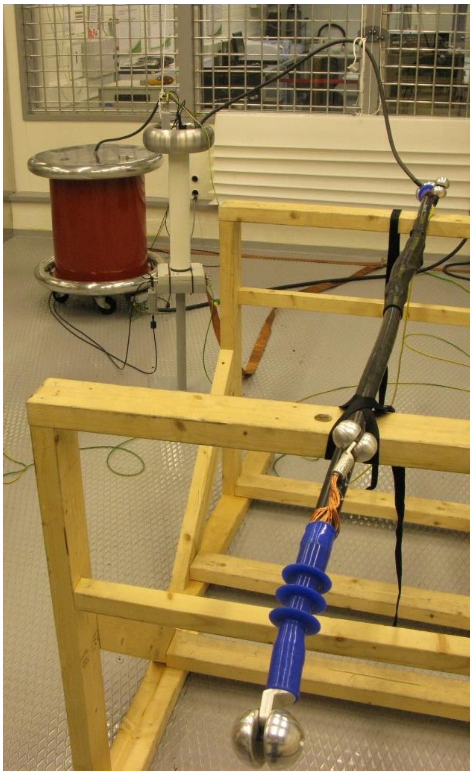

Figure 31. Partial discharge test setup.

The test setup is presented in Figure 31.

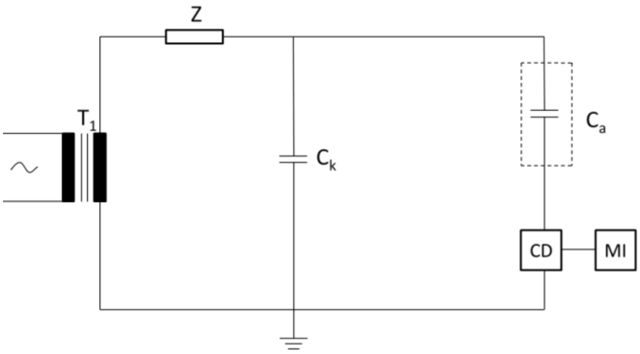

Figure 32. Test setup circuit. Adapted from Aro et al. (2011) [5 ,472].

The basic principle of the test setup can be seen in Figure 32, where T_1 is a test transformer, Z is a filter, C_k is a coupling capacitor, C_a is the test object, CD is a coupling device and MI is the measuring instrument. The test results of the partial discharge test are completely represented in Appendix 3.

8.1.2 AC Voltage Step Test

All the test lines were subjected to the AC voltage step test after the partial discharge test. The purpose of this test was to find the weakest point of the test line. In this test the AC voltage was increased with 12 kV (U_0) steps with 5 minutes hold at each voltage step until the breakdown occurred. The test was also ended when the flashovers between the termination lug and the shield wires started occur. The results of this test do not tell the complete truth about the weakest point or the seriousness of the installation errors because the thermal effects are the major determinant of the breakdown due to the short time and the high voltage. However, this test was used because the development of the partial discharges to the breakdown takes a long time. The test results of the AC voltage step test are completely represented in Appendix 4.

9 Analysis of the Results

The evaluation of the joint condition is not simple because the test requirements and the procedures are not clearly standardized. In the design and the production tests of the new medium voltage accessory, the maximum discharge level allowed at two times U_0 is 10 pC. But there is no reference of what is an allowable level of the partial discharge in the in-service accessories. Because of this, the network utilities often tend to replace the joints where the discharges are detected at the operating voltages. Sometimes the urgent replacing is unnecessary because the failures are unlikely to occur in short to medium term and the possible failure effects are minor. For example if the medium voltage cable joint with the low levels of the partial discharge activity is detected from a ring type network, monitoring the PD activity can be sufficient action. However this type of decision making requires a lot of experience and knowledge of the behavior of used products.

It is important to understand that no one is able to predict the lifetime of the insulation accurately because there are so many unknown determining variables like the defect type, the exact place of the discharges, the development of the discharge channel and the remaining insulation thickness. Therefore the following analyses that are made from the results for these specific joint types are only my own opinions.

9.1 Reference joints

The partial discharge inception voltages of the reference joints were in the simulations:

- Heat shrink joint 33 kV
- Cold shrink joint 102 kV

According to the laboratory tests the PDIV value of the studied defect free heat shrink is on the range between 30 and 35 kV depending highly on the stress control mastic quality. The inception voltage of the defect free cold shrink joint is not reached in the laboratory tests because the highest used PD testing voltage is 42 kV. The higher voltages are not tested because the flashovers at the terminations can destroy the fragile PD measuring instruments. Therefore could be said that the simulation results of the defect free joints are approximate. [31]

9.2 Fault Type 1: Irregularities on the Surface of the Cable Insulation

In this work the irregularities which were made on the surface of the cable insulation are deep. Usually in the real life joints, the left irregularities are smaller, but the edges of these cavities are usually sharper and therefore the air voids are likely. Also along with careless heating of heat shrink tube air voids are even more likely.

9.2.1 Heat Shrink Joint

The electrical test result of the HJ11.2403C joint with the irregularities on the surface of the cable insulation are represented in Table 3.

Table 3. Electrical test results of the HJ11.2403C joint with the irregularities on the surface of the cable insulation.

Sample	Partial discharge test			AC voltage step test	
	Inception voltage U_i [kV]	Discharge level at U_i [pC]	Extinction voltage U_e [kV]	Breakdown voltage [kV]	Remarks
1	14.5	430	13.0	84	Flashover at termination
2	14.0	530	12.0	72	Breakdown at termination
3	12.0	39	11.0	84	Flashover at termination

None of these joint samples broke down during the AC voltage test. Joints were opened and visually examined after the tests. Two of the joints did not have any visual signs of the discharging, but from one of the joints was found a visible electrical tree which is shown in Figure 33. The size of this electrical tree indicates that the break-down was close to occur.

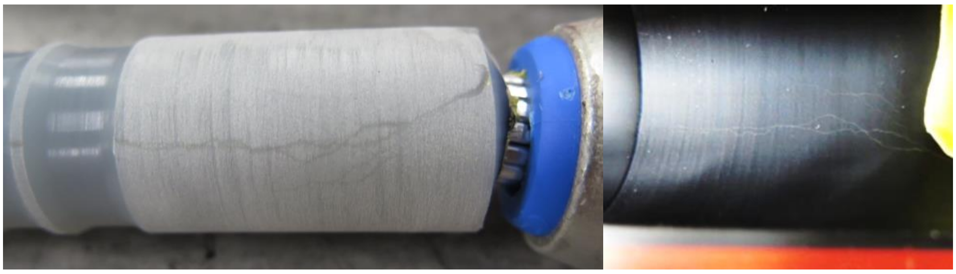

Figure 33. Electrical tree formed on the interface between the cable insulation and the joint tube on the joint sample 3.

According to the test results, this type of defect would possibly have effect to the lifetime of the cable joint in question. If these joints are not supplying electricity to anything highly critical, monitoring the development of the PD activity is sufficient action, because the inception voltages were over the operating voltage on two joints and on the remaining joint the discharge level was low at the operating voltage. Therefore the development to the breakdown would likely take a lot of time. With the similar medium voltage heath shrink joints that are designated to the higher voltage rates this type of defect would be more crucial, even though the layer thicknesses are greater on those joints.

The average inception voltage of the tested joints was 13.5 kV. The partial discharge inception voltage of this defect type was 11 kV in the simulation. The difference between the testing results and the simulation results can be explained by the high effect of the shape and the insulation thickness. The shapes of the voids in the simulation and in the tested joints are likely different.

9.2.2 Cold Shrink Joint

The electrical test result of the CJH11.2403C joint with the irregularities on the surface of the cable insulation are represented in Table 4.

Table 4. Electrical test results of the CJH11.2403C joint with the irregularities on the surface of the cable insulation.

Sample	**Partial discharge test**			**AC voltage step test**	
	Inception voltage U_i [kV]	**Discharge level at U_i [pC]**	**Extinction voltage U_e [kV]**	**Breakdown voltage [kV]**	**Remarks**
1	>40	-	-	72	Breakdown at termination
2	>40	-	-	48	
3	29.5	900	20.5	72	Breakdown at termination

Only one of the joints broke down during the AC voltage step test. The breakdown voltage of this joint was very low compared to what another two samples withstood. No visual discharge signs were found on the two joints that withstood the AC voltage step test without the breakdown. On the sample 2, the breakdown occurred between the connector electrode and the joint shield. Figure 34 shows the opened joint sample 2.

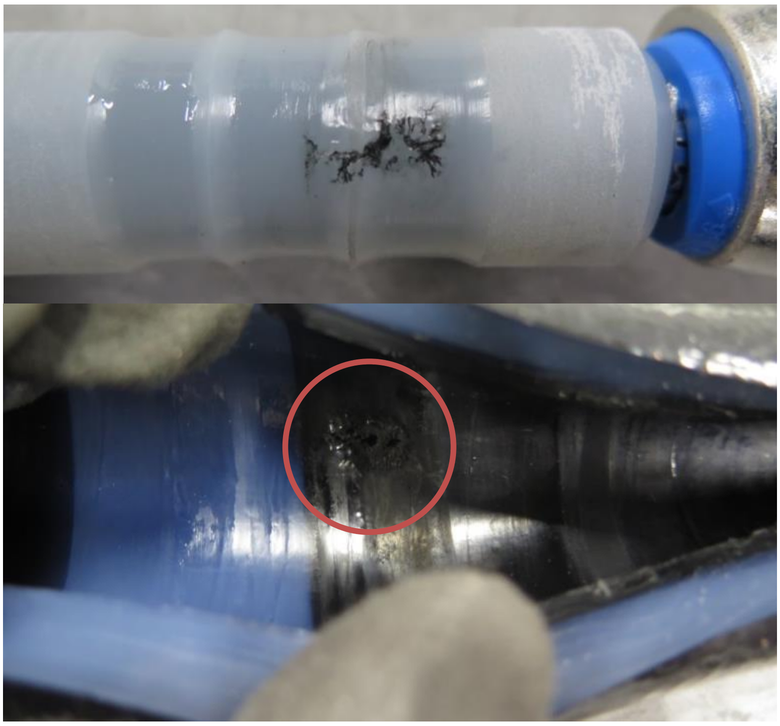

Figure 34. Breakdown marks on the joint sample 2.

Some melting of the cable insulation had also occurred below the breakdown point on the sample 2. A clear conclusion about what caused this breakdown cannot be made, but perhaps the air void was left below the connector electrode which caused the temperature rise and finally it led to the thermal breakdown. Other possible reasons are the manufacturing defect or the cut on joint body caused by the installation error.

On the PD test, the inception voltages of the two joints were not reached. On the third joint the PDIV was 29.5 kV. The high discharge level and the fingerprint characteristics of the partial discharge indicate that the discharges are likely caused the by air void in this sample.

The partial discharge inception voltage was 13 – 45 kV in the simulation with the air voids. Based on the results of the tests and the simulation, the conclusion is that at least one of the samples had air voids between the cold shrink joint body and the cable insulation. This type of defect would not likely have significant effect to the lifetime of the cold shrink joint in this situation because the partial discharge inception voltages were over the operating voltage. With higher operating voltage or different cable diameter the defects could cause problems more likely.

9.3 Fault Type 2: Air between the Heat Shrink Tubes

The electrical test result of the HJ11.2403C joint with the air cavities between the heat shrink tubes are represented in Table 5.

Table 5. Electrical test results of the HJ11.2403C joint with the air cavities between the heat shrink tubes.

Sample	Partial discharge test			AC voltage step test	
	Inception voltage U_i [kV]	Discharge level at U_i [pC]	Extinction voltage U_e [kV]	Breakdown voltage [kV]	Remarks
1	7.0	350	6.5	48	
2	6.5	2000	5.5	60	
3	7.5	2600	5.0	60	

All the joints broke down at the AC voltage step test. The breakdowns were expected because the insulation thickness was reduced by the grinding. The Figure 35 shows the breakdown marks left on the samples 2 and 3.

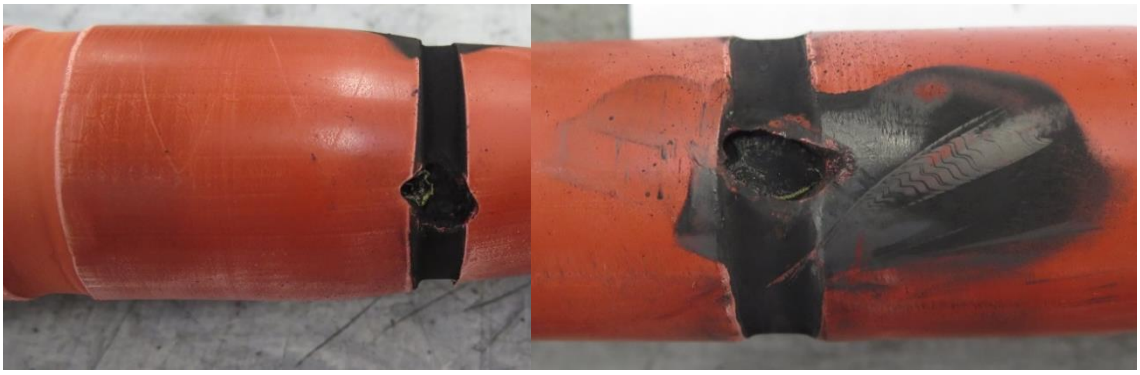

Figure 35. Breakdown marks on the joint samples 2 and 3.

The average inception voltage was 7.0 kV on the partial discharge test. In the simulation, the partial discharge inception voltage was 6 kV. The difference between the testing results and the simulation results can be explained by the high effect of the shape and the insulation thickness. This type of defect would have significant effect to the lifetime of the joint because the partial discharge inception voltages were much lower than the operating voltage and the discharge levels were high. Because of the high level of discharging, the discharge levels were not measured at the operating voltage.

9.4 Fault type 3: Faulty Positioning of Cold Shrink Joint Body

The electrical test result of the CJH11.2403C joint with the faulty positioning of the joint body are represented in Table 6.

Table 6. Electrical test results of the CJH11.2403C joint with the faulty positioning of the joint body.

Sample	Partial discharge test			AC voltage step test	
	Inception voltage U_i [kV]	Discharge level at U_i [pC]	Extinction voltage U_e [kV]	Breakdown voltage [kV]	Remarks
1	39.0	10	37.0	58	
2	>40	-	-	50	
3	>40	-	-	71	

Breakdown occurred between the connector electrode and the insulation screen on all the samples. On the sample 2, a hole through the cable insulation was also found close to the cut edge of the insulation screen. This hole formed the conducting path between the conductor and the insulation screen. Figure 36 shows the breakdown marks left on the sample 2. The hole through the cable insulation is circled. The conductive path between the insulation screen and the connector electrode is below the hole.

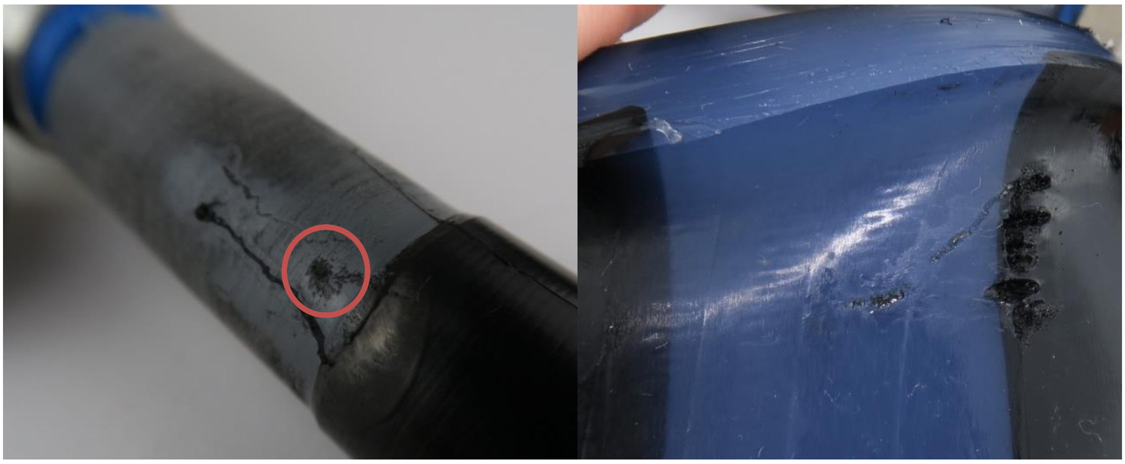

Figure 36. Breakdown marks on the joint sample 2.

The PDIV was 39 kV on one of the joints. A clear conclusion about what caused this discharging cannot be made because on the other two samples, the inception voltages were not reached. For example this type of discharging can be a consequence of small metal particles on top of the cable termination. It is also possible that the dielectric strength of the cable insulation was reached on this sample at the cut edge of the insulation screen. According to the simulation, the partial discharge inception voltage was 41 kV. This indicates that the defect has caused the discharges. To confirm this assumption, the PD testing with the higher voltage would be required. However, it would be too risky to do with the used equipment as the breakdown in the joint could break fragile measuring instruments.

This type of defect would not likely have significant effect to the lifetime of the cold shrink cable joint because the partial discharge inception voltages were over the operating voltage. The effect to the lifetime would be more significant with higher operating voltage. This type of defect could also cause problems with different cable diameter.

10 Conclusion

The aim for the thesis was to study how the installation errors effect on the medium voltage cable joints in the electrical terms and to value the seriousness of the examined installation errors in the used medium voltage joints with the simulations and the electrical tests. The aim was also to evaluate the accuracy of the simulation results in comparison with the electrical test results.

The results clearly indicate that the most vulnerable types of the defects to the partial discharges are the ones that include the air voids because the air has low dielectric strength. The magnitude of the electric field peak inside the air void depends highly on few characters. The shape of the air cavity highly effects on the field strengths, on the sharp corners the field strength is higher than on the round corners. The magnitude of the field peaks also increases when the surrounding insulation thickness is decreased. If the air void is located near to the sharp electrode surface, the electric field is naturally higher also inside the void.

With the faulty positioning of the cold shrink joint body, which does not include the air voids, the inception voltages were higher than in the defects that included the air voids. Therefore this type of defect is more unlikely to cause discharging in medium voltage joints. Based on the small difference between the partial discharge inception voltages and the breakdown voltages in the AC step test, development from the partial discharging to the breakdown in this defect type would likely be faster than with the air void defect. This is probably the result of more centralized electrical stress and without the air voids, the discharges effect more directly to the insulating material.

Based on the results, Ensto's cold shrink joints are more reliable than the heat shrink joints because the cold shrink joints are less vulnerable to the air voids caused by the installation errors. The field distribution inside the cold shrink joint body is smoother and also the dielectric strength of the insulation of the cold shrink is higher. However, because of weaker mechanical strength, the cold shrink joints are more vulnerable to the other types of defects which were not studied in this thesis.

The similarity of the simulation results and the partial discharge test results shows that the simulation results are approximate and the simulating is great tool for different tasks in the product development. The problematics can be found with the simulation and the results can be represented in an accessible form. However, the simulations are not exact because all the components were ideal without any microscopic defects and loss factors in the simulations. Also on made simulations, a lot of simplifying was done to save time and effort. In reality, the material properties have been found to vary greatly between different batches and the permittivity is not constant like it was assumed to be in the simulations. In addition, some of the shapes that have high effect to the stress distribution are hard to model accurately.

In the future, the effects of adding more physical conditions, like the current and the dielectric losses, to simulation could be studied. The usage of the simplified 3D models could be approached also in the simulations.

References

1 Toward error-free cable installations. 2014. Ensto Group. <http://www.ensto.com/newsroom/articles/101/0/toward_error-free_cable_installations>. Cited 30.11.2015.

2 Mäkelä, Mikko; Mäkelä, Riitta & Siltanen, Olavi. 2002. Insinöörikoulutuksen fysiikka 2. Tampere: Tammertekniikka.

3 Lehto, Heikki & Luoma, Tapani. 1998. Fysiikka 4. Helsinki: Kirjayhtymä Oy.

4 Wolfson, Richard. 2014. Essential University Physics Volume 2. Essex: Pearson.

5 Aro, Martti; Elovaara, Jarmo; Karttunen, Matti; Nousiainen, Kirsi & Palva, Veikko. 2011. Suurjännitetekniikka. Helsinki: Otatieto.

6 Naidu, M. S. & Kamaraju, V. 2004. High Voltage Engineering. New Delhi: Tata McGraw-Hill.

7 IEC 60270 High-voltage test techniques – Partial discharge measurements. 2000. International Electrotechnical Commission.

8 About Partial Discharge. IPEC Ltd. <http://www.ipec.co.uk/about-partial-discharge/>. Cited 10.11.2015.

9 COMSOL Multiphysics. COMSOL Inc. <http://www.comsol.com/comsol-multiphysics>. Cited 23.11.2015.

10 Elovaara, Jarmo & Haarla, Liisa. 2011. Sähköverkot II. Helsinki: Otatieto.

11 HD 620 S2 Distribution cables with extruded insulation for rated voltages from 3,6/6 (7,2) kV up to and including 20,8/36 (42) kV. 2010. GENELEC – European Committee for Electrotechnical Standardization.

12 DRYREX Korkealaatuiset keskijännitekaapelit. Reka Cables Ltd. <http://www.reka.fi/sites/default/files/media/Brochures/965_korkealaatuisetkeskijnnitekaapelit.pdf>. Cited 25.11.2015.

13 Medium voltage cable AHXCMK-WTC 20 kV 1-core. Reka Cables Ltd. <http://www.rekacables.com/medium-and-high-voltage-cable/medium-voltage-cable/medium-voltage-cable-ahxcmk-wtc-20-kv-1-core>. Cited 25.11.2015.

14 HD 629.1 S2 Test requirements on accessories for use on power cables of rated voltage from 3,6/6(7,2) kV up to 20,8/36(42) kV Part 1: Cables with extruded insulation. 2006. CENELEC – European Committee for Electrotechnical Standardization.

15 Illias, H. A.; Lee, Z. H.; Bakar, A. H. A. & Mokhlis, H. 2012. Distribution of electric field in medium voltage cable joint geometry. 2012 IEEE International Conference on Condition Monitoring and Diagnosis 23–27 September 2012, Bali, Indonesia.

16 Pictures: © Ensto Group. Downloaded 26.11.2015.

17 Ensto Pro Training Academy material: Solutions for Underground Cable Networks. Ensto Utility Networks.

18 Eigner, Alexander & Semino, Sepehr. 2013. 50 Years of Electrical-Stress Control in Cable Accessories. IEEE Electrical Insulation Magazine vol.29, no.5. September-October 2013.

19 Moore, G. F. 1997. Electric Cables Handbook, Third Edition. Oxford: Blackwell.

20 HJ11.2403C Product Card. 2015. Ensto Finland Oy. <http://products.ensto.com/catalog/product/15791/HJ11.2403C_ENG1.pdf>. Cited 26.11.2015.

21 CJH11.2403C Product Card. 2015. Ensto Finland Oy. <http://products.ensto.com/catalog/product/30689/CJH11.2403C_ENG1.pdf>. Cited 26.11.2015.

22 Electrical resistivity and conductivity. Wikipedia. <https://en.wikipedia.org/wiki/Electrical_resistivity_and_conductivity>. Cited 9.11.2015.

23 COMSOL Multiphysics material library.

24 Polyethylene Borlink™ LE4201R Crosslinkable Insulation Compound Product Data Sheet. 2015. Borealis AG. <http://www.borealisgroup.com/en/polyolefins/products/Borlink/Borlink-LE4201R/>. Cited 9.11.2015.

25 Dielectric Constants at 20°C. HyperPhysics. <http://hyperphysics.phy-astr.gsu.edu/hbase/tables/diel.html>. Cited 9.11.2015.

26 Polyethylene Visico™ LE0540 Silane Crosslinkable Semiconductive Compound Product Data Sheet. 2015. Borealis AG. <http://www.borealisgroup.com/en/polyolefins/products/Visico/Visico-LE0540/>. Cited 9.11.2015.

27 Electric property measurements. Ensto UN Product Development.

28 Heat Shrinkable Dual Layer Insulating/Semi-Conductive Tube Specification. 2012. Ensto.

29 Aarnio, Anssi. 2015. Product Development Engineer, Ensto Utility Networks, Porvoo. Conversation 30.11.2015.

30 Alkila Kauko. 2015. Claim report I-28128. Ensto UN Product Management.

31 Laboratory Test ID 2116. 2013. Ensto UN Laboratory.

HJ11.24 Installation Instructions

Saves Your Energy

ENSTO

INSTALLATION INSTRUCTION PEM1091ENG
2012-10

ENGLISH

HEAT SHRINK JOINTS FOR SINGLE CORE CABLES
HJ11.12 AND HJ11.24

GENERAL INFORMATION

- Check that the kit is suitable for the cable type.
- Check that the materials listed in the bill of materials for completeness.
- Read the installation instructions carefully before starting the operation.
- Install carefully and make sure that the materials are clean during the installation.

GENERAL INSTRUCTIONS FOR HEAT SHRINKING

- Please note that in some working places a hot work permit is needed.
- Use a propane burner with flame length of approx. 20-30 cm. Do not use too large or sharp flame.
- Move the flame all around the cable on the shrinking direction. Move the flame continuously to avoid overheating.
- Make sure that the ventilation is good and there are no flammable materials around.
- Clean the cable surfaces before shrinking.
- When shrinking, always follow the installation instructions and the relevant sequence to avoid trapped air.
- Check that the tube has shrunk evenly around the cable before you continue shrinking.
- If the tube turns around at the end of shrinking, straighten the tube by directing the flame inside the tube from the opposite direction.

LEGAL NOTICE

- The product must be installed only by a competent person with sufficient training in installation practices and with sufficient knowledge of good safety and installation practices in respect of electrical equipment. If local legislation contains provisions in respect of such training or sufficient knowledge in respect of installation of electrical equipment such provisions shall be fulfilled by the said person.
- Ensto accepts no liability concerning claims resulting from misuse, incorrect installation or ignored national safety regulations or other national provisions.
- WARNING: Failure to follow the installation instructions may result in damage to the product and serious or fatal injury.

HJ11.12 AND HJ11.24

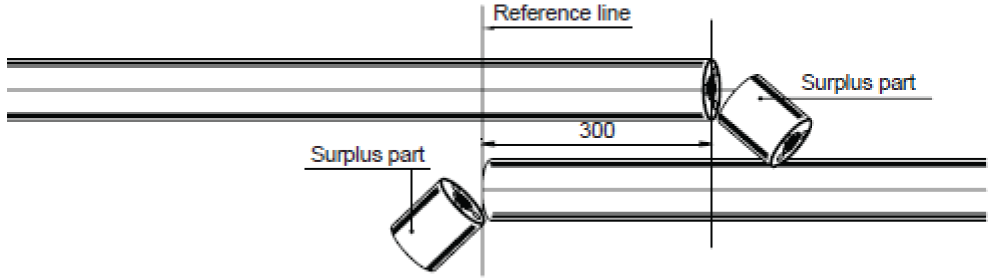

1. Overlap the cables for approximately 1 m. Mark the cables in the middle of the overlap (reference line). Cut the other cable end from the marked reference line. To ensure the shield wires are long enough, cut the other end of the cable 300 mm away from the reference line mark towards the end of the cable.

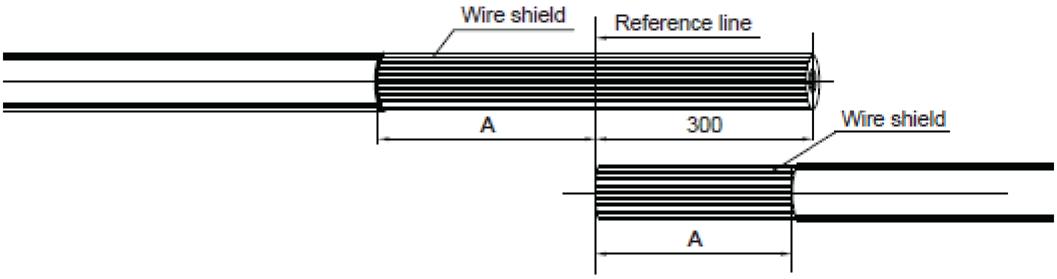

2. Cut and remove the outer sheath according to the dimension shown in table 1. Use A for the other side of the joint and A+300 mm for the other. Clean the outer sheath for 1.5 m to keep the internal surface of the heat shrink tubes free of dirt.

TABLE 1
CABLE PREPARATION DIMENSIONS

Kit	Um kV	Cable size mm^2	Outer sheath removal A mm	Semiconductive layer removal B mm	Max. connector dimensions	
					length mm	diameter mm
HJ11.1202	12	25-95	240	150	130	25
HJ11.1203	12	95-240	240	150	130	33
HJ11.1204	12	150-300	270	180	180	38
HJ11.1205	12	400-630	320	220	250	52
HJ11.1206	12	800-1000	360	260	290	65
HJ11.2402	24	25-95	280	170	130	25
HJ11.2403	24	95-240	280	170	130	33
HJ11.2404	24	150-300	310	200	180	38

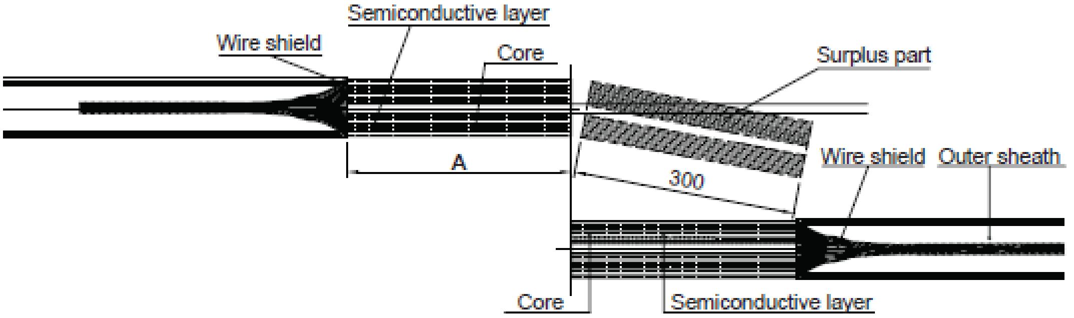

3. Do not cut the copper shield wires. Fold them over the outer sheath and fix them temporarily with PVC tape. Cut away 300 mm of the cores on the longer side.

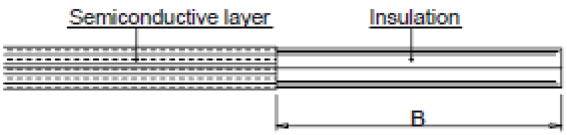

4. Remove B mm (see table 1) of the semiconductive layer measured from the end of the conductor. If the semiconductive layer is not strippable by hand, use a suitable tool. If necessary, remove any remainings of the semiconductive layer with a piece of glass. Use the grinding paper included in the kit to smooth the insulation.

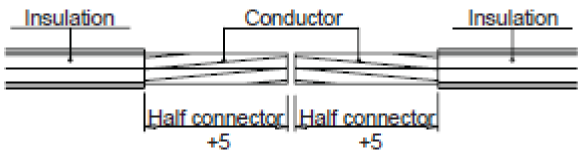

5. Remove half of the bolt connector length + 5 mm from the insulation of the cable. Be careful not nick the conductor. If you use compression connectors, remove the insulation according to connector manufacturer's instructions. Clean the conductors. Wrap a couple of layers of PVC tape around the end of the conductors.

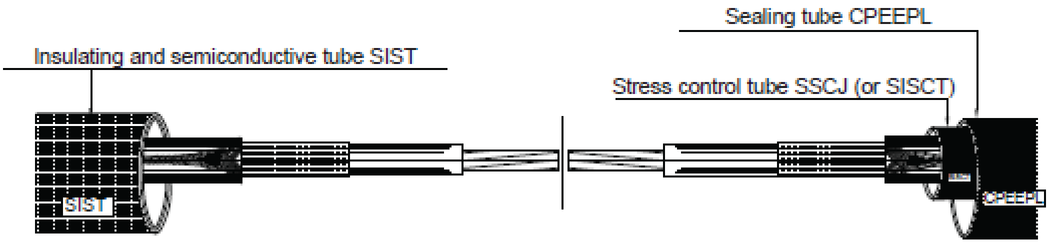

6. Slip the heat shrinkable tubes on the cables. Protect them from dirt.

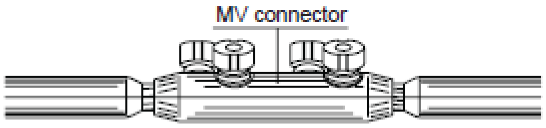

7. Remove the PVC tape from the ends of the conductors and install the MV connector following the manufacturer's instructions. Remove any sharp edges. Fill any holes left in the connector with grey mastic.

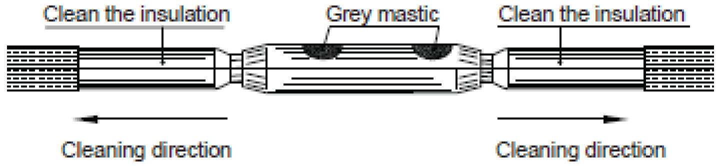

8. Clean the cable insulation with a cleaning tissue. Go towards the semiconductive layer. If necessary clean the semiconductive layer, and finally clean the semiconductive layer without touching the insulation. Thus that no semiconductive particles are deposited on the insulation. Clean the connector.

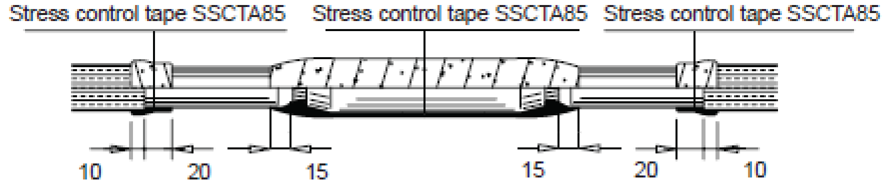

9. Fill the gap between the end of the connector and the insulation with stress control tape SSCTA85. Then wrap two layers of SSCTA85 to cover the connector. Continue up to 15 mm of the insulation on both sides. SSCTA85 must be applied with a 50% overlap and by stretching it to half of its original width.

Wrap two layers of stress control tape SSCTA85 over the edge of the semiconductive layer. Wrap SSCTA85 for 10 mm on the semiconductive layer and for 20 mm on the insulation. Start from the semiconductive side. SSCTA85 must be applied with a 50% overlap and by stretching it to half of its original width.

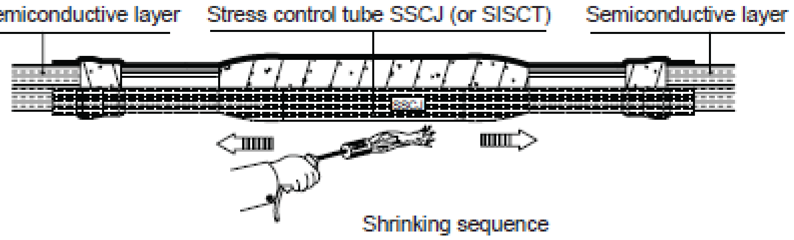

10. Centre the stress control tube SSCJ (or SISCT) on the connector. Start shrinking the tube from the middle and move towards the ends. Clean the surface of the stress control tube after shrinking.

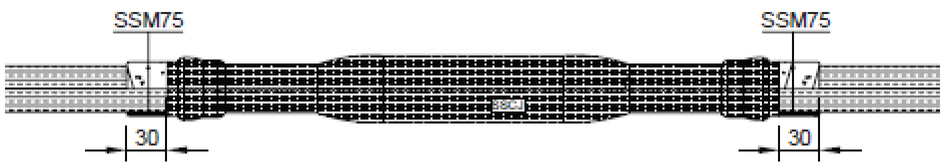

11. Wrap two layers of sealing mastic SSM75 for 30 mm length on the semiconductive layer starting from the end of the stress control tube on the both sides of the tube.

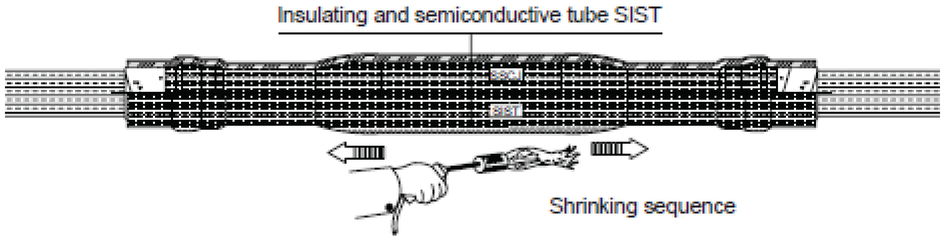

12. Centre the insulating and semiconductive tube SIST on top of the stress control tube. Start shrinking it from the middle and move towards the ends.

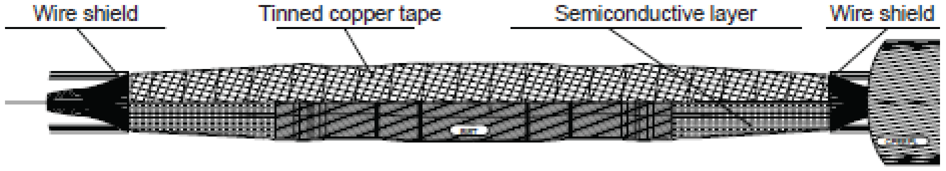

13. Wrap the core with one layer of tinned copper tape. Go from the exposed semiconductive layer on one side to the other side. Tinned copper tape must be applied with a 20% overlap. Fix the copper tape end with some PVC tape.

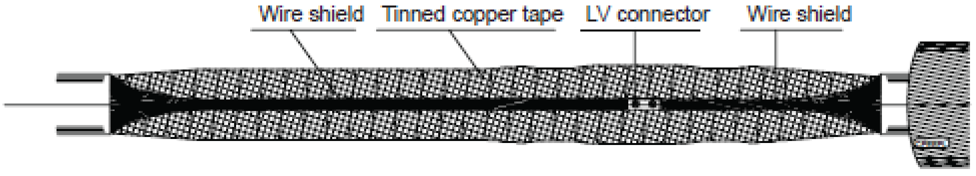

14. Twist the copper shield wires into a stranded conductor and join them with a suitable connector following the manufacturer's instructions.

HJ11.12 AND HJ11.24

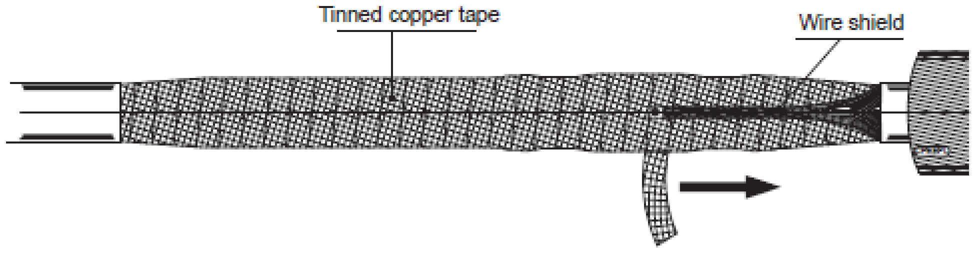

15. Wrap one layer of the tinned copper tape over the copper shield wires. Tinned copper tape must be wrapped with a 20% overlap. Fix the copper tape end with some PVC tape.

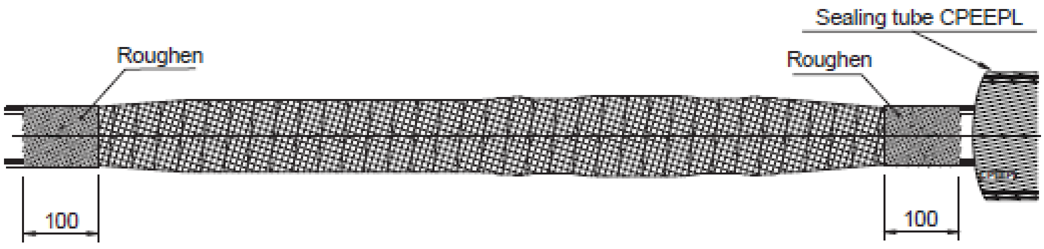

16. Roughen around 100 mm of the outer sheath on both sides of the joint with grinding paper. Treat the roughened parts gently with flame.

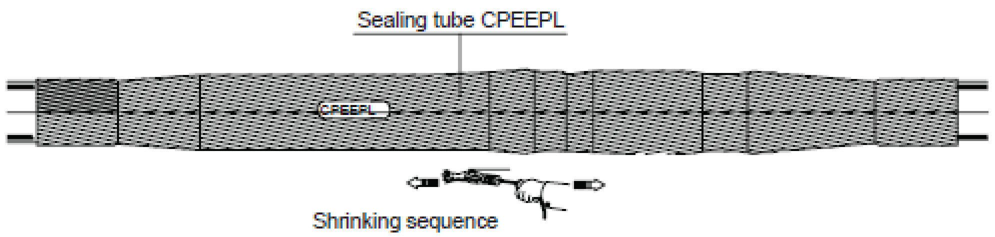

17. Centre the sealing tube CPEEPL on the joint. Start shrinking the tube from the middle and move towards the ends. The tube is properly shrunk when the adhesive starts to come out from the ends.

18. The joint is finished and ready to use, but let it cool down before loading it mechanically.

CJH11.24 Installation Instructions

Saves Your Energy

ENSTO

INSTALLATION INSTRUCTION PEM1835ENG
2015-06

ENGLISH

COLD SHRINK HYBRID JOINT CJH11.24 FOR SINGLE CORE CABLES WITH Cu WIRE SHIELD
Uo/U = 12.7/22 kV, Um = 24 kV

GENERAL INFORMATION

- Check that the kit is suitable for the cable type.
- Check the materials listed in the bill of materials for completeness.
- Read the installation instructions carefully before starting the installation.
- Install carefully and make sure the materials are clean during the installation.
- Clean the working place after the installation.

GENERAL INSTRUCTIONS FOR HEAT SHRINKING

- Please note that in some working places a hot work permit is needed.
- Use a propane burner with a flame length of approx. 20-30 cm. Do not use too large or sharp flame.
- Move the flame all around the cable on the shrinking direction. Move the flame continuously to avoid overheating.
- Make sure that the ventilation is good and there are no flammable materials around.
- Clean the cable surfaces before shrinking.
- When shrinking, always follow the installation instructions and the relevant sequence to avoid trapped air.
- Check that the tube has shrunk evenly around the cable before you continue shrinking.
- If the tube turns around at the end of shrinking, straighten the tube by directing the flame inside the tube from the opposite direction.
- After shrinking the tubes should be smooth and even following the shape inside.

LEGAL NOTICE

- The product must be installed only by a competent person with sufficient training in installation practices and with sufficient knowledge of good safety and installation practices in respect of electrical equipment. If local legislation contains provisions in respect of such training or sufficient knowledge in respect of installation of electrical equipment such provisions shall be fulfilled by the said person.
- Ensto accepts no liability concerning claims resulting from misuse, incorrect installation or ignored national safety regulations or other national provisions.
- WARNING: Failure to follow the installation instructions may result in damage to the product and serious or fatal injury.

GENERAL INSTRUCTION FOR COLD SHRINK

- Ensure the cold shrink tubing is placed upon the cable core prior to installing the connector/lug, for ease of assembly.
- When using cleaning solvents, ensure there is no residue remaining after cleaning. Solvent or other residue will impair the joint performance.
- Ensure that the plastic tape is straightened within the tube. If it is wrapped around the conductor, rotate the cold shrink assembly counter clockwise, to ensure the tape is straight, before attempting to withdraw the tape.
- Once you have correctly placed the cold shrink tube, the plastic spiral may be withdrawn with a steady pulling action. Take care to ensure the unwound spiral is not tightening around the cable. The excess spiral can be cut if required, as it is withdrawn.
- Double check the position of the tube as it begins to shrink. There is only a limited time to adjust the position of the tube

SPIRAL POSITION BEFORE BEGINNING THE SHRINKING OF THE TUBE

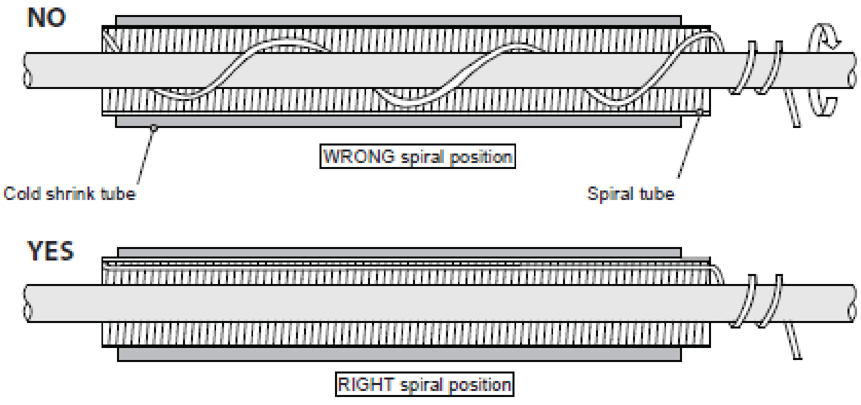

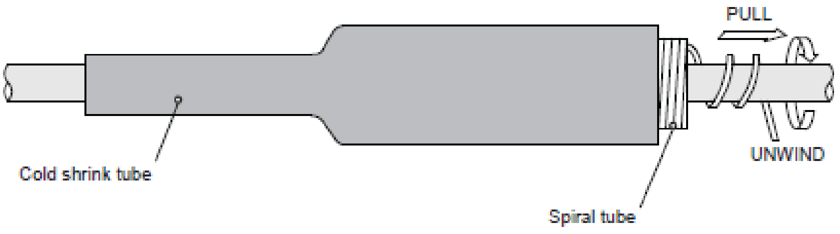

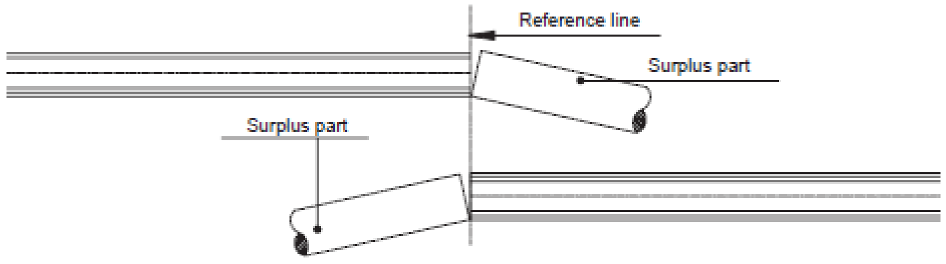

1. ☐ Check the length of each core according to the final installed position.

Table 1

Type	Min. diam. on the cable insulation mm	12 kV mm^2	24 kV mm^2	B mm	C mm	E mm
CJH11.2402C	13.8	35-95	10-95	190	155	315+-5
CJH11.2403C	18.4	95-240	70-240	175	140	285+-5
CJH11.2404C	25.3	240-300	185-240	225	190	385+-5
CJH11.2404C	25.3	-	300	220	185	375+-5
CJH11.24045C	25.3	240-400	185-240	225	190	385+-5
CJH11.24045C	25.3	-	300-400	220	185	375+-5
CJH11.2405C	31.1	400-630	400-630	220	185	380+-5
CJH11.2406C	36.8		630-800	270	235	475+-5
CJH11.2406C	36.8		1000	265	230	465+-5

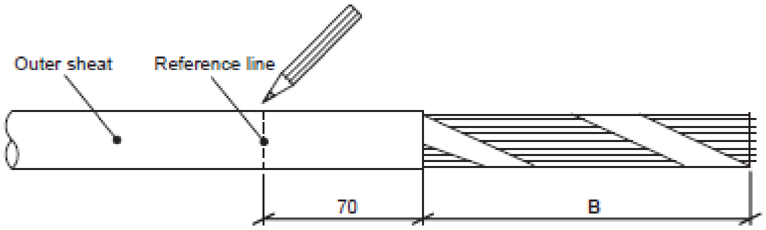

2. ☐ Remove the outer sheat for a distance of B mm from the core end.

☐ Mark a reference line 70 mm from the outer sheat cutting point.

☐ Fold back and pull together the screen wires and if needed fix them temporarily with some PVC tape.

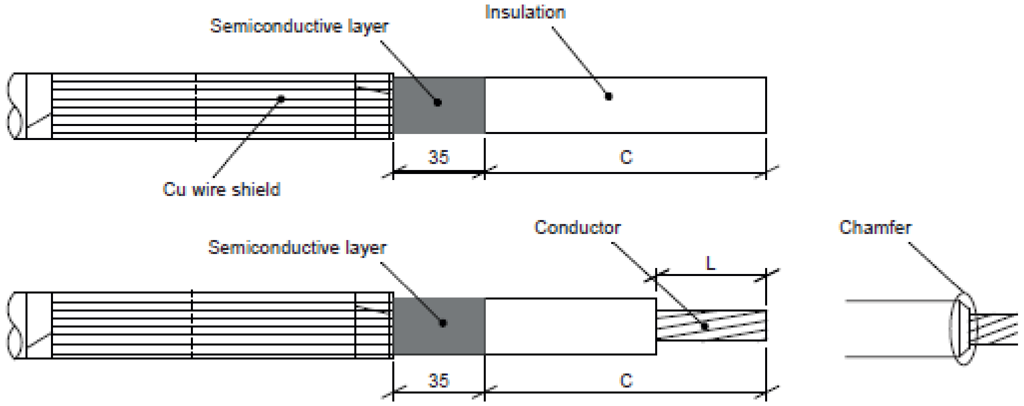

3. ☐ Using a suitable tool to remove the semiconductive layer for a distance of C mm measured from the cable end.

☐ If necessary, remove any remaining of the semiconductive layer with a piece of glass.

☐ Use the grinding paper included in the kit to smooth the insulation.

☐ Remove the insulation for a distance of L mm according to connectors installation instruction.

☐ Use the grinding paper to do a chamfering to the sharp insulation edge.

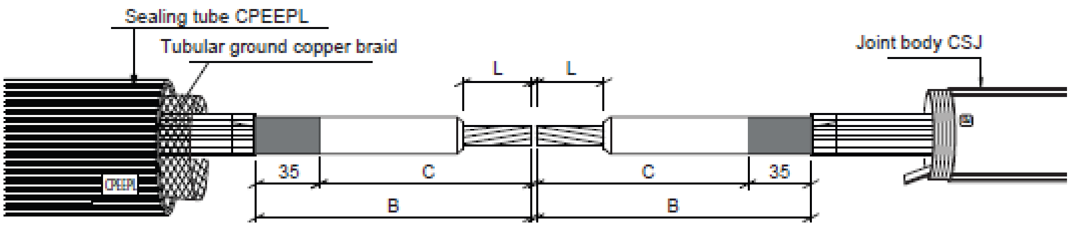

4. ☐ Place the tubular ground copper braid on the cable outer sheat.

☐ Place the sealing tube CPEEPL on the cable outer sheat.

☐ Place the joint body CSJ on the cable outer sheat.

! Protect the tubes from dirt.

5. ☐ Check measurement E before installing the connector.

☐ Install cable connectors according to the connectors installation instructions.

☐ Clean the cable insulation and the semiconductive layer with a cleaning tissue starting from the insulation and move towards the semiconductive layer. Take care that no semiconductive particles are deposited on the insulation. At last clean the connector.

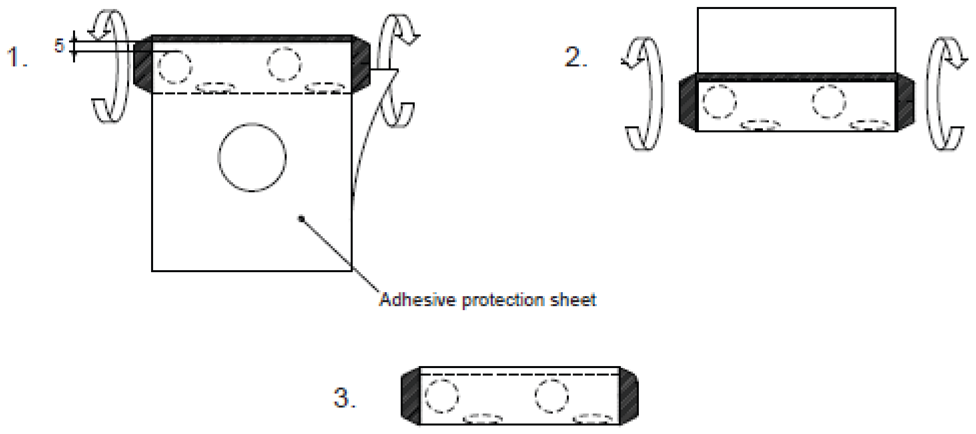

6. ☐ Remove the protective foil from the adhesive protection sheet.

☐ Place the sheet 5 mm from the first two screw holes.

☐ Continue to wrap the whole sheet on the connector.

! When wrapping is completed there should be two sheet layers on all the screw holes.

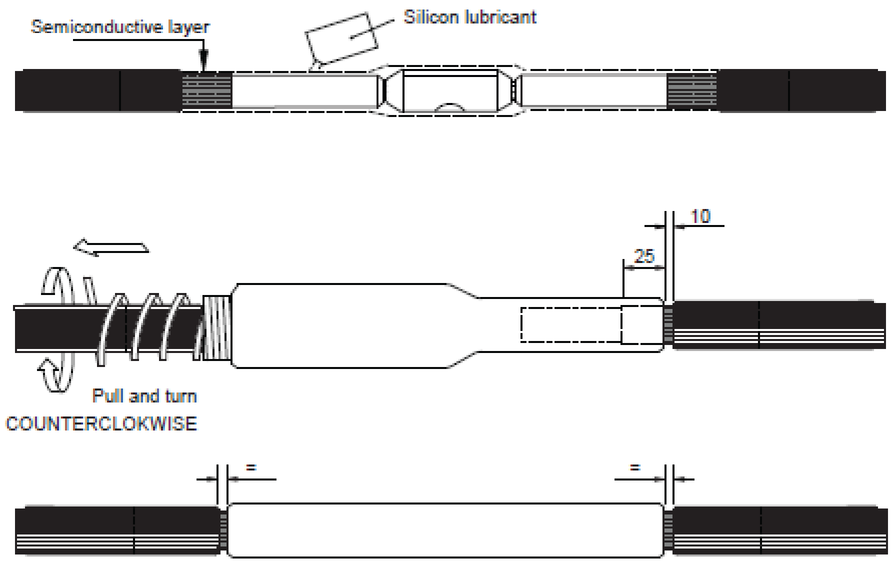

7. ☐ Spread a thin layer of silicon grease evenly over the insulation, semiconductive layer and at last over the connector.

☐ Position the CSJ joint body according to the dimensions in the picture and start pulling the spiral so that the joint body shrinks down 1-2 cm from the end. Adjust the joint body so that edge of the tube is 10 mm from the outer sheat cut.

☐ Holding the joint body, pull out the spiral gently and at the same time turning it counterclockwise.

! If necessary, at this stage, minor repositioning of the body is still possible.

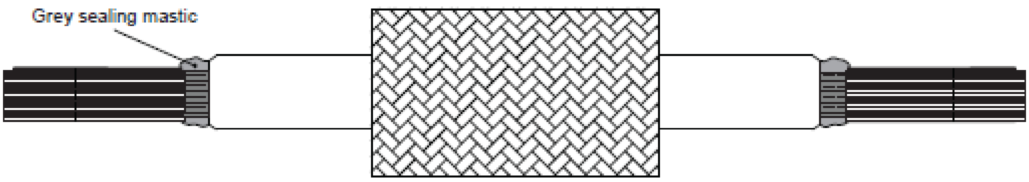

8. ☐ Fill the space between outher sheat of the cable and the joint body with some mastic on both sides of the joint, as shown in the picture.

! Make sure the mastic is applied firmly and evenly.

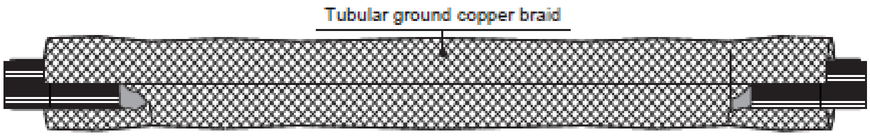

9. ☐ Position the ground copper braid over the joint so that it overlaps the shield wires.

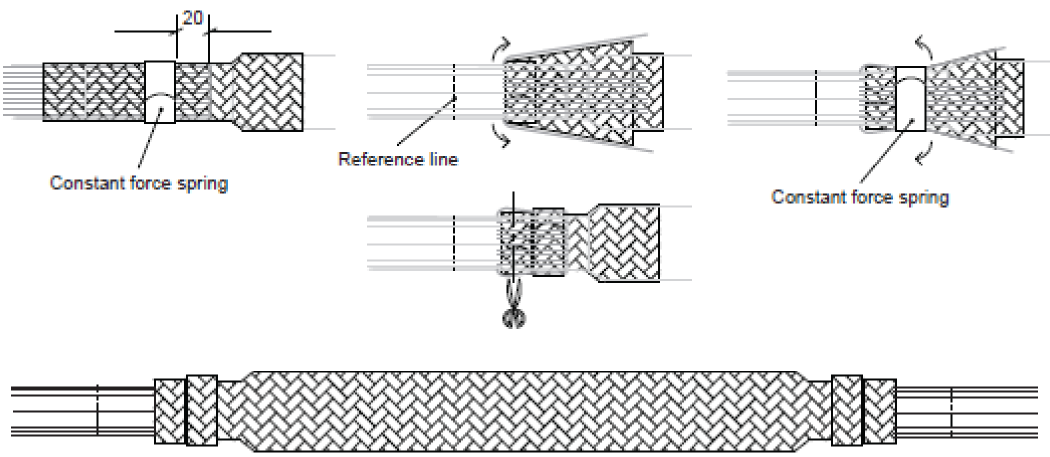

10. ☐ Position the first constant force spring 20 mm from the outer sheat cut.

☐ Fold back, over the fixed constant force spring, the shield wires and the tubular ground copper braid.

☐ Fix the second constant force spring close to the first one (as shown in the picture) and fold the shield wires and the tubular ground copper braid in the opposite direction of the previous fold.

☐ Remove the exceeding wires and braid.

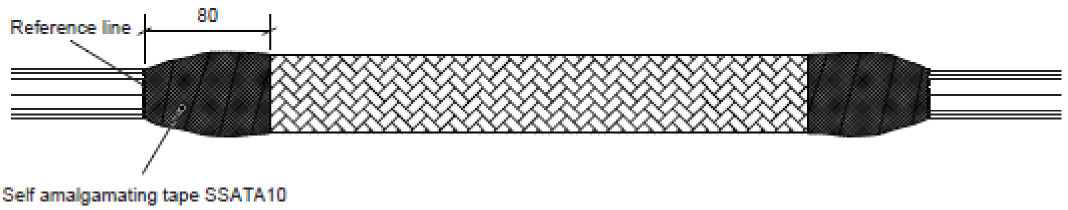

11. ☐ Apply the self amalgamating tape (SSATA10) for a distance of 80 mm starting from the reference line and moving towards the joint.

! Self amalgamating tape should be applied tightly and by stretching it to half of its original width.
! Use 1/2 roll on each side of the joint.

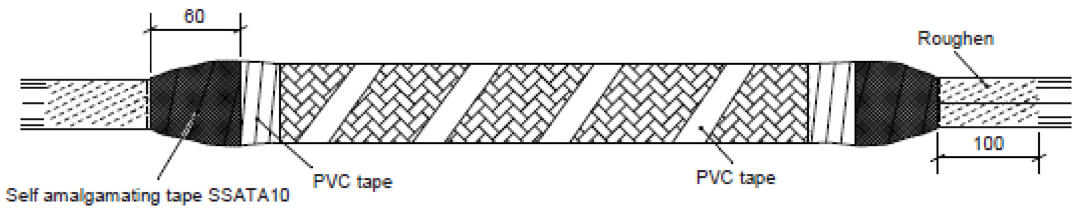

12. ☐ Use PVC tape to fasten the ground copper braid on the joint. Leave 60 mm of self amalgamating tape free of PVC tape.

☐ Roughen 100 mm of the cable outer sheat with grinding paper on both sides of the joint.

☐ Treat the roughened parts gently with flame.

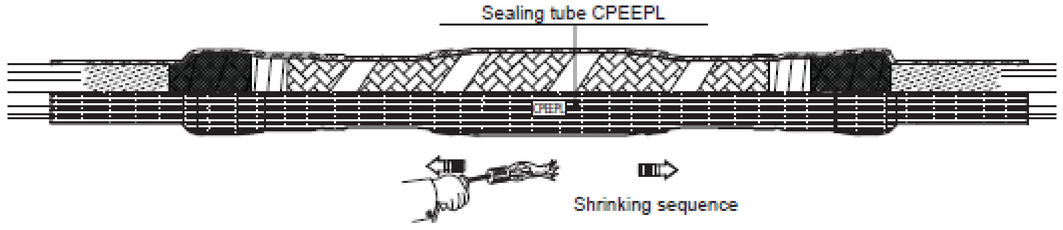

13. ☐ Centre the heat shrink tube on the joint.

☐ Start shrinking the tube from the middle and move towards the ends.

! The tube is properly shrunk when the adhesive starts to come out from the ends.

14. ☐ The joint is finished and ready to use, but let it cool down before loading it mechanically.

Partial Discharge Test Results

Partial Discharge Test

Test Id:	3465	**Used equipment:**	L22 Baur HV Test device
Testing date / tester:	11.11.2015 / SVu		L204 PDIX Charge Calibrator
			L206 PDIX PD-Meter
Test lines:			L207 PDIX HV-Control unit
Line 1-3:	Fault type 1: Irregularities on the Surface of the Cable Insulation, Heat Shrink Joint		L208 Coupling capacitor
Line 4-6:	Fault type 1: Irregularities on the Surface of the Cable Insulation, Cold Shrink Joint		
Line 7-9:	Fault type 2: Air Between the Heat Shrink Tubes		
Line 10-12:	Fault type 3: Faulty Positioning of the Cold Shrink Joint Body		
Cables:		**Temperature:**	21 'C
Line 1-2:	AHXAMK-WTC 1x150 mm2	**Humidity:**	36 % rh
Accessories:			
Indoor termination:	CIT1.2403L		
Heat shrink joint:	HJ11.2403C		
Cold shrink joint:	CJH11.2403C		

PD test 12/20 (24) kV

Line	Noise at minimum voltage level [pC]	Discharge level [pC]															Inseption voltage Ui [kV]	Discharge level [pC] at inception voltage	Extinction voltage Ue [kV]
		6 kV	6,5 kV	7 kV	8,5 kV	12 kV	15 kV	18 kV	20 kV	22 kV	24 kV	30 kV	33 kV	36 kV	38 kV	40 kV			
1	3	3				3	430		1000	>2000							14,5	430,0	13,0
2	3	3				3	1300	1500	1700	>2000							14,0	530,0	12,0
3	3	3				39	1500	1800	>2000								12,0	39,0	11,0
4	3	3				3	3		3		3	3		3		3	> 40		
5	3	3				3	3		3		3	3		3		3	> 40		
6	3	3				3	3		3		3	1000	1100	1200			29,5	900,0	20,5
7	3	3				3	3		3		3	3		3	10	13	39,0	10,0	37,0
8	3	3				3	3		3		3	3		3		3	> 40		
9	3	3				3	3		3		3	3		3		3	> 40		
10	3	3	3	400	1650												7,0	350,0	6,5
11	3	3	2800	3000													6,5	2000,0	5,5
12	3	3	1200	1600	2800												7,5	2600,0	5,0

AC Voltage Step Test Results

AC Voltage Step Test

Test Id:	3465		
Testing date / tester:	11.11.2015 / SVu		
		Used equipment:	L22 Baur HV Test device
Test lines:			L204 PDIX Charge Calibrator
Line 1-3:	Fault type 1: Irregularities on the Surface of the Cable Insulation, Heat Shrink Joint		L206 PDIX PD-Meter
Line 4-6:	Fault type 1: Irregularities on the Surface of the Cable Insulation, Cold Shrink Joint		L207 PDIX HV-Control unit
Line 7-9:	Fault type 2: Air Between the Heat Shrink Tubes		L208 Coupling capacitor
Line 10-12:	Fault type 3: Faulty Positioning of the Cold Shrink Joint Body		
Cables:			
Line 1-2:	AHXAMK-WTC 1x150 mm2		
Accessories:		**Temperature:**	21 'C
Indoor termination:	CIT1.2403L	**Humidity:**	36 % rh
Heat shrink joint:	HJ11.2403C		
Cold shrink joint:	CJH11.2403C		

AC voltage step test

Line		5 min 12 kV	24 kV	36 kV	48 kV	60 kV	72 kV	84 kV	Breakdown voltage [kV]	Remarks
1	Leakage current [mA]	2,4	4,8	7,4	9,7	12,0	13,0	16,0	84	Arcing over termination
	Time	5 min	5 min	5 min	5 min	5 min	5 min	1 min		
2	Leakage current [mA]	2,4	5,0	7,7	10,0	12,0	14,0		72	Termination failed (arcing)
	Time	5 min	5 min	5 min	5 min	5 min	1 min			
3	Leakage current [mA]	2,4	4,6	7,1	9,4	12,0	14,0	16,0	84	Arcing over termination
	Time	5 min	5 min	5 min	5 min	5 min	5 min	1 min		
4	Leakage current [mA]	2,6	5,4	8,1	10,6	12,0	15,0		72	Termination failed
	Time	5 min	5 min	5 min	5 min	5 min	20 s			
5	Leakage current [mA]	3,0	6,0	9,2	-				48	
	Time	5 min	5 min	5 min	2 s					
6	Leakage current [mA]	3,4	6,8	10,2	12,0	16,0	19,0		72	Termination failed
	Time	5 min	5 min	5 min	5 min	5 min	4 min			
7	Leakage current [mA]	2,5	5,0	7,6	10,0				58	
	Time	5 min	5 min	5 min	5 min					
8	Leakage current [mA]	3,0	5,8	8,8	12,0				50	
	Time	5 min	5 min	5 min	5 min					
9	Leakage current [mA]	2,8	5,8	8,6	12,0	14,0			71	
	Time	5 min	5 min	5 min	5 min	5 min				
10	Leakage current [mA]	2,4	4,9	7,3	9,6				48	
	Time	5 min	5 min	5 min	4 min 40 s					
11	Leakage current [mA]	2,2	4,6	6,9	9,2	12,0			60	
	Time	5 min	5 min	5 min	5 min	1 min 10 s				
12	Leakage current [mA]	2,4	4,8	7,2	9,6	12,0			60	
	Time	5 min	5 min	5 min	5 min	20 s				